UNIVERSITÀ DEGLI STUDI DI PADOVA

Dipartimento di Fisica e Astronomia "Galileo Galilei"

Corso di Laurea in Astronomia

Tesi di Laurea

Natal kick models and their impact on binary black hole formation

Relatore

Prof.ssa Michela Mapelli

Correlatore

Dott. Manuel Arca Sedda

Laureanda

Martina Cacciola

Anno Accademico 2021/2022

Abstract

Compact objects that form via core-collapse supernova explosions of the progenitors are expected to get a spatial velocity at their birth, referred to as natal kick, because of asymmetric mass ejection. For neutron stars, we can reconstruct the distribution of kick magnitudes from observations of proper motions of Galactic pulsars, but for black holes the data are scanty and complex to interpret. In this thesis work, we review the main observational hints for black hole natal kicks and study the main proposed models to describe them. In order to prove the self-consistency of these prescriptions, we present some histograms of the main parameters involved and compare the outcomes of three different distributions, underlying how the natal kick impact on binary black holes evolution still represents an open issue.

Contents

1

Introduction

1.1 Gravitational wave astrophysics for binary black hole research

Gravitational waves (GWs) are considered as ripples in the space-time continuum due to an enormous variation of the gravitational potential. One of the triggering events may be the orbital motion of extremely compact objects around a common centre, which results damped by the emission of energy. The theoretical hypothesis of the existence of GWs was introduced by Einstein's General Relativity back in 1916. The first observational evidence can be found in Hulse & Taylor (1975), who focused their work on a pulsar-neutron star binary, whose orbit shrinks according to Einstein's laws. Eventually, about seven years ago, LIGO interferometers obtained for the first time a signal (GW150914), that later was confirmed to be a gravitational wave generated by the coalescence of two black holes (BHs) with mass around 30 $M_{\odot}$ each. This detection paved the ground for a whole new branch of studies, GW astrophysics, which allows us to investigate the mechanisms that rule some of the most extreme environments in the universe. Since then, thrilling times for BBH research have followed: the latest observations had furnished crucial information about the physics of binary compact objects, but also given rise to doubts. Detections had shown that a number of BHs are able to merge within Hubble time. So far, most of the LIGO–Virgo runs involved BHs with mass over 20 $M_{\odot}$. This outcome is surprising since it exceeds both the expected value known from observation (stellar BHs, mainly from X-ray binaries, have mass under 20 $M_{\odot}$) and the prediction from the majority of theoretical models, which did not contemplate the possibility of a mass m_{BH} >30 $M_{\odot}$, apart from a few exceptions.

1.2 BHs formation from single star

Until now, it is known that BBHs exist, can reach merger by gravitational wave emission and are composed of BHs with mass ranging from few solar masses to $\sim 50 M_{\odot}$.
We will not take into account primordial BHs, whose birth is supposed to come from gravitational instabilities in the early Universe. In this thesis, we restrict our attention to stellar BHs, final remnants of the gravitational collapse of a massive star (zero-age main sequence star with $m_{ZAMS} \gtrsim 20 M_{\odot}$) that ends in a supernova (SN) explosion or in the collapse of the core. Vice versa, stars with initial masses up to 20 $M_{\odot}$ probably leave neutron star remnants. With increasing mass, the amount of kinetic energy generated by the collapse decreases, while the binding energy of the envelope increases. In case of a weak explosion, some of the material ejected may fall back onto the proto-neutron star. If accretion causes the mass to exceed the maximum possible mass of a neutron star (which is not precisely determined but lies between 2-3 $M_{\odot}$) then the proto-neutron star will collapse and form a black hole. The mass limit separating stars that form neutron stars and those that leave black holes is probably in the range 20–25 $M_{\odot}$ but is sensitive to the details of the explosion mechanism (see Figure 1.1).

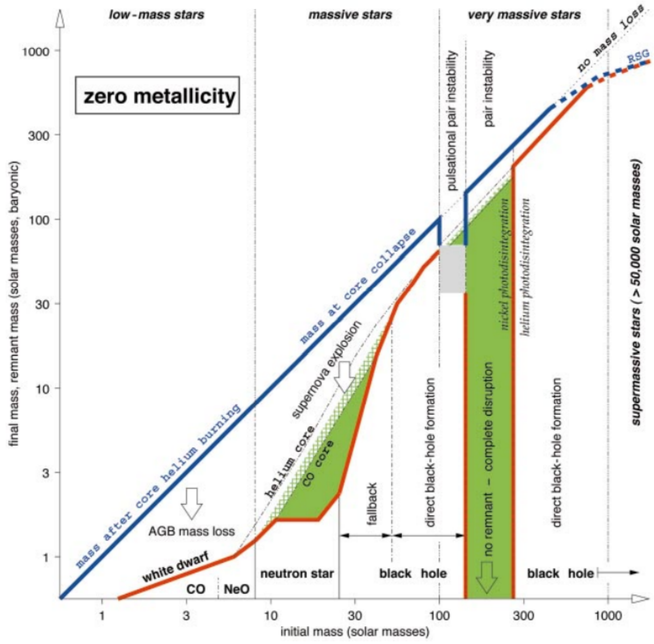

Figure 1.1: Initial mass-final mass relation for stars of solar composition (from Woosley et al., 2002 [46])

Let us linger on stellar-origin BHs before delving into the proper discussion about binaries: we are going to briefly summarise the state-of-the-art knowledge, this being essential to understand their pairing mechanism. The BHs mass function might be influenced by a number of scarcely discerned processes within the evolution of the star, so it is still rather ambiguous. Playing a key role in the subsequent formation of the compact remnant, there are both (i) mass loss by stellar winds and (ii) the type of supernova explosion.

1.2.1 Stellar winds

Stellar winds are fast-flowing streams of gas (including protons, electrons and atoms of heavier metals) that are emitted by the atmosphere of stars (with $M \gtrsim 15\ M_{\odot}$), gradually eroding their outer layers. Ejection rates, velocities and causes change with the mass of the star. Their comprehension is striking for the study of compact objects: in fact, mass loss has a key role in determining the pre-SN mass of a star at the onset of collapse and consequently the outcome of SN explosion. Indeed, the final mass of the star identifies the upper limit to the black hole mass.
For masses $M \gtrsim 15\ M_{\odot}$, mass loss by stellar winds becomes important during all evolution phases, including the Main Sequence (MS). For masses above 30 $M_{\odot}$ the mass-loss rates $\dot{M}$ are so large that the timescale for mass loss, $\tau_{ml} = M/\dot{M}$ becomes smaller than the nuclear timescale τ_{nuc}. Hence, mass loss has a very significant effect on massive star evolution, albeit the not well-determined rate $\dot{M}$ adds uncertainties in the treatment of these systems.
Cold, luminous stars, such as red giants and asymptotic giant branch (AGB) stars, experience a slow but copious stellar wind, that is probably driven by a combination of stellar pulsations and radiation pressure on dust particles formed in the cool outer atmosphere (resulting to be the same mechanism as the '*superwind*' of AGB stars). During core-He burning phase, a large part or even the entire envelope of red supergiants evaporates by the wind, exposing the helium core of the star that appears as a Wolf-Rayet (WR) star.
The situation varies if we consider massive hot stars (e.g. O and B stars, luminous blue variables and WR stars): for those objects, it takes action the electrostatic coupling of the momentum between photons and metal ions, meaning that the outer layers are accelerated outwards and the star becomes unstable. For O-B stars in the MS, mass loss depends on metallicity as $\dot{M} \propto Z^{\alpha}$, where Z is the absolute metallicity and α a factor which, according to the latest models, should change at least with luminosity. Moreover, post-MS stars present an additional term, the electron-scattering Eddington factor $\Gamma_e = \kappa_e L/(4\pi G c m)$, where κ_e stands for the electron-scattering cross section, L and m the

stellar luminosity and mass respectively. It has been established that while L gets closer to the Eddington luminosity L_{Edd} (i.e. the maximum luminosity that can be carried by radiation, inside a star in hydrostatic equilibrium), the metallicity dependence tends to be cancelled for $L \gtrsim L_{Edd}$. Therefore, we adopt a mass loss prescription considering that metallicity dependence tends to fade towards the radiation pressure-dominated region. It turns out that a solar-metallicity star could lose about 2/3 of the initial mass, in contrast to metal-poor stars able to retain almost all of the $M_{initial}$. Other factors that can enter the discussion are: surface magnetic fields, which appear to strongly quench stellar winds; rotation, leading to an increase of luminosity, thus a rise of mass loss and a smaller pre-SN mass.

1.2.2 Core-Collapse Supernovae

Since we aim to estimate as better as we can the properties of the final remnants, let us begin by distinguishing between stars that end in a core-collapse SN explosion or in a failed SN. The first ones will leave a NS or a light BH. Otherwise, if the final mass of the star is $m_{fin} \gtrsim 40 M_\odot$ direct collapse will set in, resulting in a massive BH because the outer layers are retained by such a large binding energy that cannot be overcome by the explosion.
Essentially, all types of supernova are driven by the same physical mechanism: they appear to be associated with the core collapse of massive stars (M $\gtrsim 8M_\odot$), endowed with short lifetimes and in most cases red supergiants as progenitors. The only exception is Type Ia SNe, triggered by the mass accretion of a white dwarf in a binary system with a subsequent thermonuclear explosion. Stars with $M \gtrsim 11M_\odot$ form an inner core composed of iron-group elements (mainly ^{56}Fe), soon becoming inert with no energy that can be extracted by means of nuclear fusion. The iron core is in a peculiar state of electron degeneracy, because of neutrino cooling during the late stages of evolution. Since the pressure is dominated by relativistic electrons (whose energy exceeds mc^2), a phase extremely close to dynamical instability settles in, from when contraction cannot be stopped. Not only the dynamical timescale is shortened in these conditions of high density ($\sim 10^{10}$ g/cm^3), but also the already rapid contraction is accelerated by two main processes that occur at this point: electron captures and photo-disintegration.

1. **Electron captures**: electrons with kinetic energy overcoming the difference in nuclear binding energy can be captured and bound into β-unstable heavy nuclei. This process generates a neutron-rich environment, giving rise to the so-called *neutronization*. As the number of free electrons declines, the electron pressure consequently decreases, undermining the precarious hydrostatic equilibrium and triggering the collapse. Stellar explosions caused by this mechanism are called electron-capture SNe.

2. **Photo-disintegration**: it happens when photons have gained energy large enough to break heavy nuclei bonding. In particular, ^{56}Fe is disintegrated into α-particles and neutrons. A great amount of energy is required to accomplish the process and is furnished firstly by the radiation field and eventually by the internal energy source: the number of e$^-$ is further diminished; the pressure decreases, fostering the core free-fall.

At this stage, electrons have been gradually removed, because of proton captures generating neutrons and neutrinos. So the core is predominantly made of neutrons, which build a new pressure supporting the star against collapse. Neutron gas becomes almost incompressible and in order to maintain equilibrium, the core goes rapidly from a radius of a few thousand km to a radius of a few ten km in about 10 msec. At $R_c \approx 20$ km, the mass of the central degenerate core reaches the Chandrasekhar mass (1.44 M$_\odot$): the degeneracy pressure of relativistic electrons is no longer sufficient to support it against collapse.
The gravitational energy released during the collapse of the core ([28]) can be estimated as:

$$E_{grav} \approx -\frac{GM_c^2}{R_{c,i}} + \frac{GM_c^2}{R_{c,f}} \approx \frac{GM_c^2}{R_{c,f}} \approx 3 \times 10^{53} erg \tag{1.1}$$

assuming the core having M_c equal to the Chandrasekhar mass and initial radius $R_{c,i} \sim 3000$ km. In the aforementioned equation, G is the gravity constant, while $R_{\mathrm{c,i}}$ and $R_{\mathrm{c,f}}$ are the initial and final core radii. We can compare this with the energy necessary to expel the envelope:

$$E_{env} = \int_{M_c}^{M} \frac{Gm}{r} dm \ll \frac{GM}{R_{c,i}} \tag{1.2}$$

Considering a realistic mass distribution in the envelope, we obtain $E_{env} \sim 10^{50}$ erg. Only a very small fraction of the energy released in the collapse of the core is needed to blow away the envelope. Part of the energy goes into the kinetic energy of the ejected envelope and energy radiated away by the supernova. It is possible to estimate the kinetic energy, taking into account as the mass of the ejected envelope $M_{env} \sim 10\ M_{\odot}$ and ejecta velocities 10^4 km/s: the obtained result is $E_{kin} \sim 10^{51}$ erg. Meanwhile, the total energy lost in the form of radiation is $E_{ph} \sim 10^{49}$ erg. It is clear that $E_{grav} \gg E_{kin}+E_{ph}+E_{env}$. Therefore, only a small fraction of the energy released in the collapse is used in the actual explosion. The main question is how about 1% of gravitational energy is partially converted into the kinetic energy that consents the envelope to blow out and trigger the SN explosion.
Whilst the collapsing core reaches nuclear densities ($\rho \sim 3\times\ 10^{14}$ g/cm^3), the degenerate nucleons inside cause a huge increase of the pressure. Accordingly, the so-called *core bounce* sets in: the inner part of the core bounces back like a spring, reversing the collapse. The outward motion of the inner core meets the infalling matter and then the impact generates a shock wave, whose kinetic energy was once thought to be sufficient to blow off the envelope. However, it turns out that energy absorption via photo-disintegration and electron captures is sufficient to avoid a "prompt explosion". These processes alone should have drained all the available sources, i.e. both the nuclear energy released during lifetime and the energy coming from the collapse. At this point, the shock stalls and some mechanism should intervene to make the SN happen.
Among the solutions that have been proposed so far, the most examined is the **convective SN engine**. Let us consider the neutrinos produced during the contraction: their mean free path ends to be of the typical dimension of the collapsing core, which then becomes opaque. Neutrinos can only diffuse out via many scattering events, being thereby stuck inside a 'neutrino trapping surface'. However, in correspondence with the outer layers, analogously to a star's photosphere, it can be defined as the 'neutrinosphere', outside of which low densities let the neutrinos free to escape.
Nevertheless, the neutrino transport problem can be fixed in an energy-dependence way. Their degeneracy state provokes energy high enough to be of the order of the Fermi energy of relativistic electrons, making electron capture less probable. The deposition of neutrino energy in the core provides an energy source that may revive a shock wave and give origin to the explosion. Indeed, neutrinos start diffusing out the proto-neutron star, the flux heating the region where the former shock wave has passed and causing it to become convectively unstable. Convection thus provides a way to convert some of the thermal energy from neutrino settling into kinetic energy. This process drives an outward force that can overcome the pressure of the infalling matter and launch a proper SN explosion. This engine leading to explosion with spherical symmetry works successfully only for low initial masses (up to $\sim 10\ M_{\odot}$). Otherwise, the SN fails.
Another recently proposed model suggests that the proto-neutron star might be sensible to g-mode oscillations, that create acoustic energy in the shock wave region. These acoustic waves are responsible for asymmetries in the upcoming SN explosion, whereby the core still accretes on one side while the explosion affects the other direction. These anisotropies could assign a "kick" at the birth of the compact object.

Thereupon, in order to study compact-object masses, simulations of SN explosions are built to follow the evolution of the shock; it is necessary to add artificially to the pre-SN model some amount of kinetic or thermal energy because potential asymmetries have to be taken into account. Following this pathway, O'Connor & Ott (2011, [33]) propose a criterion to establish whether a SN is successful or not, based on the compactness parameter:

$$\xi_m = \frac{m/M_{\odot}}{R(m)/1000km} \tag{1.3}$$

where $R(m)$ is the radius that enclose a certain mass m. Usually, the compactness is defined for $m = 2.5\ M_{\odot}$, corresponding to $\xi_{2.5}$. Simulations have found out that increasing $\xi_{2.5}$ means a shorter

time to generate a BH. Therefore, stars with $\xi_m > \xi_{2.5}$ are more likely to prevent an explosion and form a BH by direct collapse. It has been calculated that the best threshold between exploding and non-exploding models is $\xi_{2.5} \sim 0.2$.
Ertl et al. (2016, [8]) present a two-parameter criterion to give a better comprehension of the physics behind core-collapse SNe: their model includes M_4 as the mass of the star at the onset of the collapse and μ_4 the spatial derivative at the location of M_4.
The previous prescriptions are sometimes addressed as "islands of explodability" because they depict a scenario where there are ranges of mass where a star is expected to explode, surrounded by mass intervals in which the final fate of a star is the direct collapse. They also depend on quantities which cannot be estimated earlier than the outbreak of core collapse, requiring the use of stellar evolution models.
A plain formalism is the one from Fryer et al. (2012, [12]). They suggest that the mass of the compact remnant depends mostly on two quantities: the carbon-oxygen core mass and the total final mass of the star m_{fin}. In particular, $m_{\rm CO}$ helps to assess if the star will undergo a core-collapse SN or a direct collapse in a BH (for $m_{CO} \geq 11$ M$_\odot$), whereas $m_{\rm fin}$ defines the amount of fallback on the proto-NS. In this scheme, the time to launch the shock is the only free parameter and has a significant influence on the explosion energy. The energy appears reduced if the shock is launched $\gg 250$ ms after the start of the collapse (*delayed SN explosion*) with respect to an explosion launched in the first ~ 250 ms (*rapid SN explosion*).
Apart from any of these models, even if we could tell which end is reserved for a given star, the final mass of the compact object would still be not precisely determined. In the case of a failed SN, the main uncertainty is represented by the fate of the envelope. Indeed, the envelope of a massive star is so loosely bound that even a small energy injection is able to unbind a fraction of it. One of the mechanisms accountable for the ejection of the stellar envelope may be neutrino emission during the proto-NS phase, which ends up in a sound wave travelling out of the star as a shock.
The analysed prescriptions seem to portray a scenario where stars with larger final masses and carbon-oxygen cores (e.g. metal-poor stars), that retain most of their envelope, prove higher binding energy and thereby are more expected to result in a direct-collapse BH.

1.2.3 Pair instability and mass gap

Another phenomenon becomes effective in threatening the stability of massive stars and in even causing their end, in particular for helium cores $\gtrsim 30$ M$_\odot$ and core temperature $\gtrsim 7 \times 10^8$ K at the end of carbon burning. At very high temperatures and relatively low densities, a photon may turn into an electron-positron pair if its energy $h\nu$ exceeds the rest-mass energy of the pair $2m_ec^2$. Pair production takes place at a temperature $T \sim 10^9$ K since the number of energetic photons is already large enough to create pairs. The newly created positrons tend to be annihilated quickly: this means that an increase in temperature leads to a growth in the number of particles at expense of the energy of the photons. It induces subsequently a drop in radiation pressure supporting the star against gravitational collapse. Then, a runaway process might begin: whilst the carbon-oxygen core contracts, more energy of γ-rays is absorbed, enhancing both pair production and annihilation, until inward pressure can be able to overwhelm the outward term.

For $m_{He} > 135$ M$_\odot$, there is no way to reverse and stop the contraction, which provokes the direct collapse into a BH. If $135 \gtrsim m_{He} \gtrsim 64$ M$_\odot$, the overpressure is sufficient to favour the collapse and to trigger the sudden nuclear fusion of heavier elements (such as oxygen, neon and silicon), followed by a thermonuclear explosion. The outcome is a pair-instability SN (PISN), after which the star is completely disrupted and no compact remnant is left behind. According to predictions, this process contributes to the "**upper mass gap**" in the mass distribution of BHs (see Figure 1.2) between approximately ~ 50 and 120 M$_\odot$. The boundaries of the gap are subject to great uncertainty due to the lack of a full understanding of the physics of massive stars (e.g. doubts about nuclear reaction rates or the role of stellar rotation).
Smaller helium cores ($\sim$ 32-64 M$_\odot$) undergo pulsational PI, that drives oscillations in the core due to the softened equation of state. The star loses a small amount of mass during each oscillation till a

new equilibrium is reached with a lower core mass. At the end of this phase, there will still be a BH, but lighter than what is expected without pair instability.

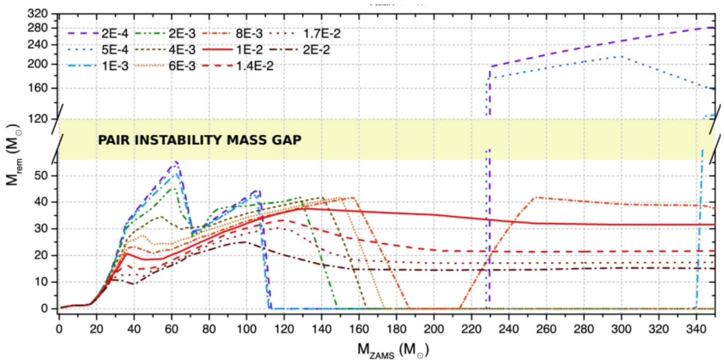

Figure 1.2: Predicted compact object mass (M_{rem}) as a function of the zero-age main-sequence (ZAMS) mass of the progenitor star (M_{ZAMS}) for 11 different metallicities. Pulsational pair-instability and pair-instability SNe are included. (Adaptation from Figures from Spera & Mapelli 2017, [39])

1.3 Binary BHs formation: environment and processes

In the previous section, we discussed about BHs coming from single progenitor stars. In the majority of cases, BHs actually evolve in binary systems with very short orbital separation. During the life of a close and isolated binary star, several processes can interfere, changing irretrievably its final fate. Mass transfer, common envelope and natal kicks shall be included among the noteworthy ones.

1.3.1 Mass transfer and Common Envelope

If a star in a binary system has orbital separation going from a few hundred to a few thousand solar radii, there is a chance for the two stars to exchange matter with each other. This flow may be driven either by stellar winds or by an episode of Roche-lobe filling.
While a massive star undergoes mass loss because of **stellar winds**, its companion could acquire a fraction of this mass. The accretion rate is easily determined thanks to Hurley et al. (2002,[20]), using the amount of mass loss suffered by the donor and the relative velocity of the wind with respect to the companion star:

$$\dot{m}_2 = \frac{1}{\sqrt{1-e^2}} \left(\frac{Gm_2}{\nu_{\rm w}^2}\right)^2 \frac{\alpha_{\rm w}}{2a^2} \frac{1}{[1+(\nu_{\rm orb}/\nu_{\rm w})^2]^{3/2}} |\dot{m}_1| \tag{1.4}$$

where e is the binary eccentricity, m_2 is the mass of the accreting star, $\nu_{\rm w}$ is the velocity of the wind, $\alpha_{\rm w}$ an efficiency constant, a the semi-major axis of the binary, $\nu_{\rm orb}$ is the orbital velocity of the binary and $\dot{m}_1$ is the mass loss rate.
The **Roche lobe** of a star in a binary system is the maximum equipotential surface around the star, within which matter is still bounded. The only intersection between the two lobes is the Lagrangian L1 point. Mass transfer is generally more efficient with respect to the action of stellar winds: it happens in case of a larger radius when the star overfills its Roche-lobe and transforms into a giant. A simple representation can be found in Figure 1.3. The approximated shape concerning a star with mass m_1 is:

$$R_{L,1} = a\frac{0.49q^{2/3}}{0.6q^{2/3} + \ln{(1+q^{1/3})}} \tag{1.5}$$

where a is the semi-major axis of the binary and $q = m_1/m_2$ (with m_2 is the mass of the star companion).

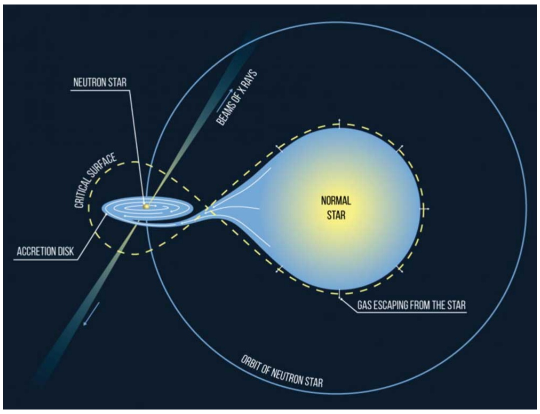

Figure 1.3: A binary system where the normal star has filled its Roche lobe.

Mass transfer changes the masses of the two stars involved and consequently the final mass of the compact remnant and its orbital properties. When a star expands faster than the Roche lobe or both stars overfill their Roche lobe, the mass transfer becomes dynamically unstable: at this point, the binary is expected to merge or to enter **common envelope** (CE).
The two stellar cores are embedded in the same non-corotating envelope, caught in a spiral as an effect of gas drag exerted by the envelope. Some of the orbital energy lost by the cores contributes to heating the envelope and in making it loosely bound. If we consider this loss as the only energy requested to unbind the envelope, the α formalism ([44]) permits to establish the fraction of orbital energy that actually contributes:

$$\Delta E = \alpha(E_{\mathrm{b,f}} - E_{\mathrm{b,i}}) = \alpha \frac{G m_{\mathrm{c1}} G m_{\mathrm{c2}}}{2} \left(\frac{1}{a_{\mathrm{f}}} - \frac{1}{a_{\mathrm{i}}} \right) \tag{1.6}$$

where $E_{\mathrm{b,i}}$ ($E_{\mathrm{b,f}}$) is the orbital binding energy of the two cores before (after) the CE phase, a_{i} (a_{f}) is the semi-major axis before (after) the CE phase, m_{c1} and m_{c2} are the masses of the two cores, and α is a dimensionless parameter that measures which fraction of the removed orbital energy is transferred to the envelope.
After the common-envelope phase, discrimination is needed whether the envelope is ejected or not, in sight of a further study of the evolution (as explained in Figure 1.4). If there is the ejection, the binary survives, made of the BH and the naked helium core of the giant and with a shorter orbital separation (corresponding to a semi-major axis equal to $\sim$ 1-100 $R_{\odot}$). If the naked helium core becomes a BH, the system evolves in a BBH that will be able to merge within Hubble time. On the other hand, if the envelope is not ejected, the two cores merge into a single BH at a premature time, with no binary left.

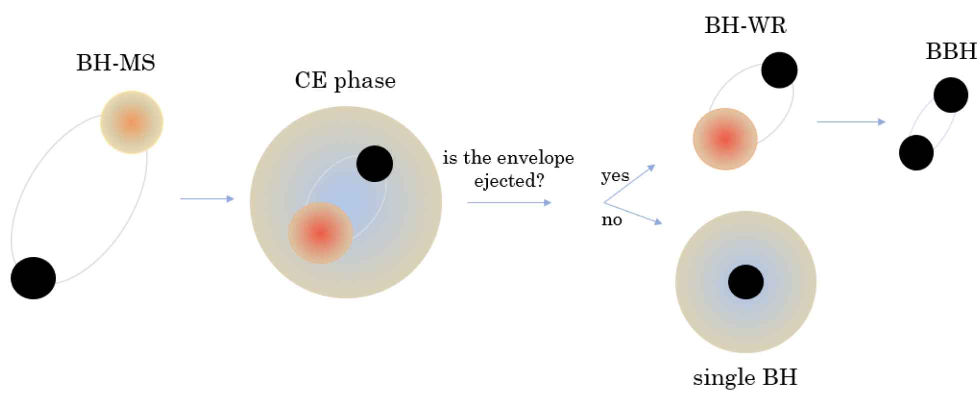

Figure 1.4: A simple cartoon depicting the evolution of a binary system, subject to a common envelope (based on the work in Mapelli 2021, [25]).

2

Natal Kicks

Compact objects are expected to obtain a spatial velocity at their birth from the parent SN explosion, referred to as **natal kick**, due to asymmetries in the neutrino emission and/or in the ejecta ([21] for more details). It is crucial to understand the physics and the statistics behind this phenomenon because natal kicks can affect significantly the evolution of a binary compact object, with the possibility to either unbind the binary or change its orbital properties (as the mass loss provides a net momentum in the rest frame of the system). They can also affect the merger rate density and provide effective probes to distinguish between birth pathways. Several works have made progress in portraying a formalism for natal kicks of neutron stars (NSs) and black holes. For example, the prescription proposed by Giacobbo & Mapelli ([13]) can naturally account for differences between core-collapse, electron-capture and ultra-stripped SNe (i.e. explosions of naked helium stars previously stripped by their compact companion).
The knowledge about NSs is definitely wider: the received kicks from core-collapse SNe are in the range $\sim$ 200-400 km/s. On the basis of observational estimates of pulsar proper motions, two main distributions have been proposed: a Maxwellian distribution with root-mean-square velocity σ=265 km/s (a simplification to single star evolution, Hobbs et al., [18]) or a bimodal velocity distribution (Fryer et al., [11] and Arzoumanian et al., [1]) with a first peak at low velocities ($\sim$ 0 km/s according to [11] or 90 km/s according to [1]) and a second one at high velocities ($\sim$ 500 km/s in [1] or >600 km/s in [11]). Although the engine leading to the formation of the compact object is roughly the same, the study concerning BHs is filled with uncertainties: whether BHs are subject to natal kicks, to what extent and which distribution fits better the data is still a matter of debate.
In the treatment of BHs, it is important first to establish if the BH comes from fallback or direct collapse. The former case gives birth to lighter BHs, whose natal kicks resemble the same distribution as NS kicks but are corrected either for linear momentum conservation ([24]) or the effect of fallback ([12]). The latter produces massive BHs, resulting extremely gravitational bound and thus no kick is usually assumed apart from **Blaauw kick** ([4]). If the SN occurs in a binary star, even if the mass loss is completely symmetric, a non-negligible kick is expected to affect the orbital properties of the binary system. It has to be attributed solely to the rapid mass loss succeeding the SN explosion and is given by the expression:

$$v_{\rm mlk} = \frac{\Delta M}{M'}\frac{M_2}{M}\sqrt{\frac{GM}{a}} \tag{2.1}$$

with M as the total mass of the binary at the onset of the SN explosion, M' the total mass of the binary after the explosion, ΔM as the mass lost (i.e. $\Delta M = M - M'$), M_2 the mass of the secondary and a the binary semi-major axis at the beginning of the explosion. If the binary remains bound, it means that the mass loss must be $< 0.5(M_{\rm He} + m)$, where $M_{\rm He}$ is the mass of the progenitor helium star and m is the mass of the donor star. In the general case, the mass of the compact remnant is given by $m_{\rm rem} = m_{\rm proto} + m_{\rm fb}$, where $m_{\rm proto}$ is the mass of the proto-NS and $m_{\rm fb} = f_{\rm fb}(m_{\rm fin} - m_{\rm proto})$ is the mass accreted by fallback (with $m_{\rm fin}$ being the mass at the onset of the collapse and $f_{\rm fb}$ the fallback parameter).
In order to embrace the complexity of natal kicks, the following relation is needed to calculate the magnitude of the kick $v_{\rm kick}$ and is based on the linear one proposed by Bray & Eldridge ([7] and [6]) $v_{\rm kick} = \alpha(m_{\rm ej}/m_{\rm rem}) + \beta$:

$$v_{\rm kick} = f_{\rm H05}\frac{m_{\rm ej}}{\langle m_{\rm ej}\rangle}\frac{\langle m_{\rm NS}\rangle}{m_{\rm rem}} \tag{2.2}$$

where f_{H05} is a normalization factor drawn by the Maxwellian distribution by Hobbes et al. ([18]) named before (H05), m_{ej} ($\langle m_{ej} \rangle$) is the (average) ejected mass of the SN, associated with the formation of a NS of mass $\langle m_{NS} \rangle$. The ejecta mass (as the difference between the final mass of the star and the remnant mass) is taken into account for the effects of asymmetries and the mass of the compact object is important to keep in mind linear momentum conservation, due to which greater masses are related to smaller kicks.

It is possible to define a second prescription, independent of m_{rem}, to check the impact of the mass of the compact object on kicks:

$$v_{kick} = f_{H05} \frac{m_{ej}}{\langle m_{ej} \rangle} \tag{2.3}$$

2.1 Prescriptions in population synthesis simulations

Following the approach described before, Giacobbo & Mapelli ([13]) have run a set of simulations based on four different models: *Ej1* which implements kicks according to Equation 2.2, *Ej2* whose natal kicks are drawn from Eq. 2.3, *H105* that refers to the Maxwellian from [18] including both CCSNe and ECSNe with a correction for the fallback, and σ15 drawing natal kicks from a Maxwellian with σ=15 km/s. Results at solar metallicity can be seen in Figure 2.1, where the break on the x-axis consents to show BHs formed from core-collapse, thus with zero natal kick.

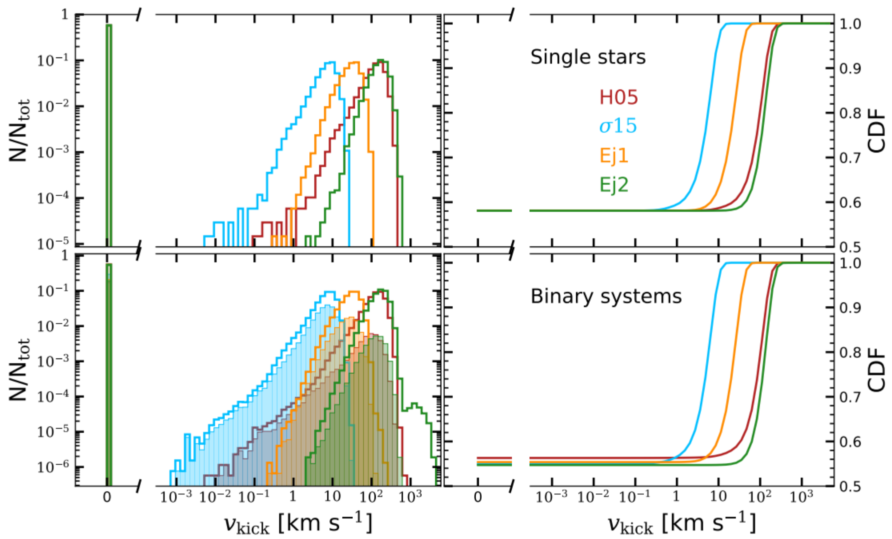

Figure 2.1: Left-hand panels: distribution of natal kicks for all BHs from single-star evolution (top) and binary-star evolution (bottom) at Z=0.02. Right-hand panels: cumulative distribution of natal kicks for all BHs (from [13]).

It turns out that, in case of single-star evolution, all the models predict that $\sim$ 60% of BHs have progenitors that collapsed directly, since no kick has been detected. The rest of the sampling receives a kick. Binary evolution has a different effect on BH kicks: in fact, dissipative mass transfer changes m_{rem}, producing smaller BHs. In this way, the decrease in the percentage of BHs that experience no kick is easily explained.

For each set of binary simulations, it can be computed the merger efficiency, i.e. the number of compact-object mergers in a certain population, within a Hubble time, divided by the total mass of the system. The **merger efficiency** η is:

$$\eta = f_{bin} f_{IMF} \frac{N_{merg}}{N_{tot,sim}} \tag{2.4}$$

where f_{bin}=0.5 is added to correct the fact that $\sim$ 50% of the stars in the model are single and f_{IMF}=0.285 takes into consideration the initial mass function, aiming to include the total mass of stars. These correction factors are necessary since the simulations only involve massive binaries.

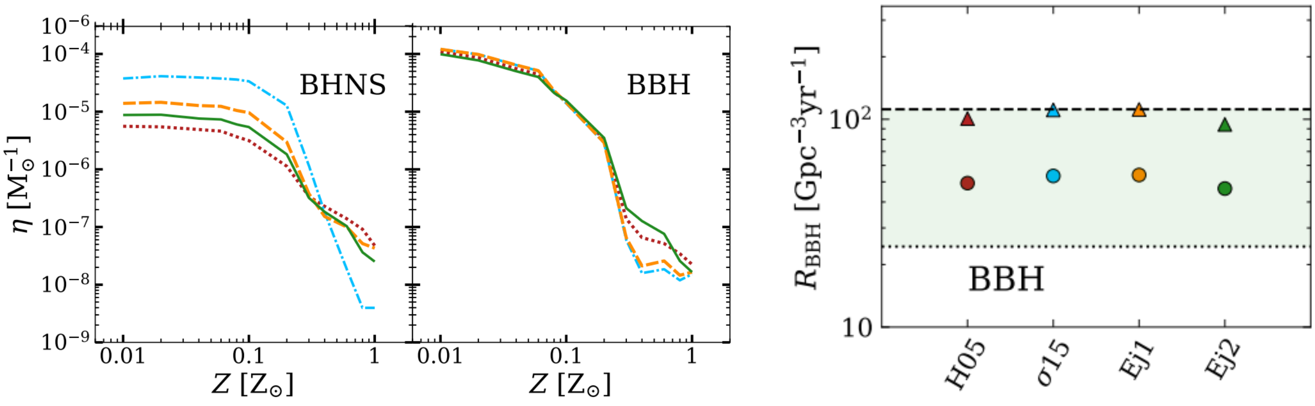

Figure 2.2: Left panel: Merger efficiency η as a function of the progenitor's metallicity for all sets of simulations (left: BHNSs, right: BBHs, from [13]). Right panel: Local merger rate density of BBHs (R_{BBH}) from [13].

In Figure 2.2 (right panel), it is evident the strong dependence of the merger efficiency of both BBHs and BHNSs on metallicity: BH mergers are at least two orders of magnitude more common in a metal-poor population than in a metal-rich one. The decrease of η with increasing metallicity can be explained with reference to the mechanism of the common envelope, which causes high-metallicity stars to rapidly lose their envelope. In this way, the binary does not have time to shrink enough to merge within a Hubble time. At intermediate metallicities, premature mergers of the progenitors are accountable for the further decrease of η.

The **local merger rate density** R is determined thanks to the equation below (from [14] and [40]):

$$R = \frac{1}{H_0\, t_{\mathrm{lb}}(z=0.1)} \int_{z_{\max}}^{z_{\min}} \frac{f_{\mathrm{loc}}(z{,}Z)\mathrm{SFR}(z)}{(1+z)\mathcal{E}(z)} dz \tag{2.5}$$

where SFR(z) is the star formation rate density, $t_{\mathrm{lb}}(z=0.1)$ is the look-back time at redshift z = 0.1, and $f_{\mathrm{loc}}(z,Z)$ is the fraction of merging systems that formed at a given redshift z and merge in the local Universe ($z \leq 0.1$) per unit solar mass. We assume $z_{\max}$= 15 and $z_{\min}$= 0. In $\mathcal{E}(z)$=$[\Omega_{\mathrm{M}}(1+z)^3+\Omega_\Lambda]^{1/2}$, H_0, Ω_M and Ω are the cosmological parameters.

The term $f_{\mathrm{loc}}(z,Z)$ has an important dependence on metallicity (that evolves with time) and is calculated from Eq. 2.4, assuming that stars at the same redshift are characterized by the same metallicity. The cosmic evolution of metallicity $D18$ is modelled in a way to resemble the fit of damped Lyman-α absorbers. This last model could be adapted in the case of the average local metallicity $Z(z=0) \sim Z_\odot$.

The population-synthesis models match the data inferred from GW170817, except for an unusual value of the parameter α in Equation 1.6, hinting at some aspects of common envelope treatment that deserve further investigation. The main outcome of the work is that BH kicks are generally **lower** than the NS ones, because of larger m_{rem} and smaller m_{ej}, meaning massive newly-born compact objects.

2.2 Observed Low-mass X-Ray Binaries distribution

Analysing the location of binaries within the Galaxy, the large distances above the Galactic plane are hard to explain without resorting to natal kicks. Nonetheless, they are not formally required to produce the system as observed, their inclusion in the treatment assists in interpreting more readily the data. Since isolated stellar-mass BHs are difficult to observe, black hole X-ray binaries (BHXBs) are used as probes to understand the BH birth mechanism in a binary system. Repetto et al. (2012, [36]) based their work on this hint, considering the population of black hole low mass X-ray binaries (BH-LMXBs) and comparing the known distances to those obtained from simulations. The distribution in our Galaxy is expressed in cylindrical coordinates: in R, i.e. the radial distance from the Galactic

centre, and in z, the distance from the Galactic plane.
Kicks can deeply affect the orbital trajectories, that can be computed starting from the model proposed for the Galactic potential ϕ (divided into its three components: the disc ϕ_{d}, the spheroid ϕ_{s} and the halo ϕ_{h}). The equations of motion are integrated from the following equations:

$$\frac{dR}{dt} = v_r, \quad \frac{dv_r}{dt} = -\left(\frac{\partial \phi}{\partial R}\right)_z + \frac{{j_z}^2}{R^3}$$
$$\frac{dz}{dt} = v_z, \quad \frac{dv_z}{dt} = -\left(\frac{\partial \phi}{\partial z}\right)_R$$

where j_z is the z-component of the angular momentum of the binary and ϕ=ϕ_d+ϕ_s+ϕ_h. The resulting typical kick velocities that the binary receives when the primary explodes as a SN are $\sim$ 200 km/s, namely a comparable speed to the circular orbital one in the Galaxy (the so-called *conspiracy of three velocities*). Integrating the aforementioned equations over a time of $\sim$ 10 Gyrs and assuming the system was born right in the Galactic plane with a perpendicular velocity $v_\perp$, we can deduce typical values of z_{max} reached. The integration is performed by replacing different values of the magnitude $v_\perp$ and of the initial position R_t. Speeds $\geq$ 200 km/s are explicable by means of the kicks. Furthermore, resuming the common envelope engine (described in subsection 1.3.1), after the system has reached an orbital separation of $\sim$ 10 $R_\odot$, mass loss kicks are of the order of 20-40 km/s for bound binaries. Kicks of this size are not enough for the highest z observed. Therefore, in these cases, the natal kick assigned to newly-formed BHs or NSs works as an additional source of energy, which supports the increase in the velocity detected. With the assumption of random direction of the natal kick, the latter v_{nk} combines with the mass loss kick v_{mlk} (in 2.1) as follows:

$$v_k = \sqrt{\left(\frac{M_{\mathrm{bh}}}{M'}\right)^2 v_{\mathrm{nk}}^2 + v_{\mathrm{mlk}}^2 - 2\frac{M_{\mathrm{bh}}}{M'} v_{\mathrm{nk,x}} v_{\mathrm{mlk}}} \tag{2.6}$$

where v_{mlk} and M' are the same quantities in 2.1, M_{bh} is the black hole mass, and v_{nk} is the velocity acquired through natal kick. We assume the x axis is aligned with the orbital speed of the BH progenitor and the y axis along the line connecting the two stars at the moment of the SN explosion. Various distributions have been proposed to model natal kicks, as shown in Figure 2.3. Hansen & Phinney (1997,[17]) came up with a Maxwellian distribution peaked at 300 km/s. Conversely, Arzoumanian et al. (2002,[1]) suggested a bimodal distribution with the lower peak at $\sim$ 100 km/s and the higher peak at $\sim$ 700 km/s. These two models have also been modified by assuming the momentum received by a BH is the same as the one imparted on a NS (**momentum-conserving kicks**, MCK). Thus, a reduction factor (enlisting the ratio between NS and BH masses) is added in the computation of kick velocities: $v_{\mathrm{nk,bh}} = (M_{\mathrm{ns}}/M_{\mathrm{bh}})v_{\mathrm{nk,ns}}$. As a consequence of a greater binding mass, BHs also have a larger probability with respect to NSs to remain bound after the primary explodes.

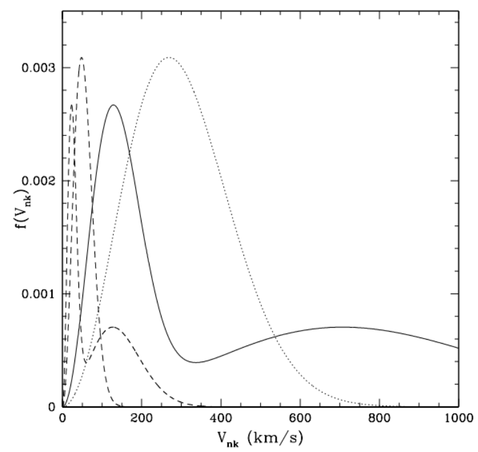

Figure 2.3: Natal Kick distributions used in binary population synthesis calculations in [36]. Solid line corresponds to Arzoumanian distribution, dotted line to Hansen & Phinney and the two dashed lines to these two distributions but with kick speeds reduced.

2.2.1 Binary population synthesis

Repetto et al. (2012, [36]) carried on the population synthesis of BH-LMXBs, considering their formation within the Galactic disc and taking as known the initial distribution of progenitor systems, their binary properties (orbital separation, from the results of common envelope evolution, and stellar masses) and the natal kick distributions for the black holes formed. In this regard, BHs natal kicks are drawn from five different distributions: four of these have already been mentioned in the previous paragraph (Hansen, Arzoumanian, and the two with MCK), the other one includes zero natal kick. The gained velocity is added randomly to the Galactic circular velocity of the binary and the orbit is integrated over the typical main-sequence time of the 1.5 $M_\odot$ companion ($\sim 3 \times 10^9$ yrs). This chosen time might be higher than the actual age of some binaries, for example, because of angular momentum losses. We then plot the positions of the 100 binaries in Galactic cylindrical coordinates, at random times of the trajectory, and compare them to the observed ones (as depicted in Figure 2.4). It is evident how the mass-loss kicks alone cannot account for the z-distribution of the observed binaries. The percentage of binaries that reach z higher than 1 kpc is low for all the models, settling down to values between 0% and 2%.

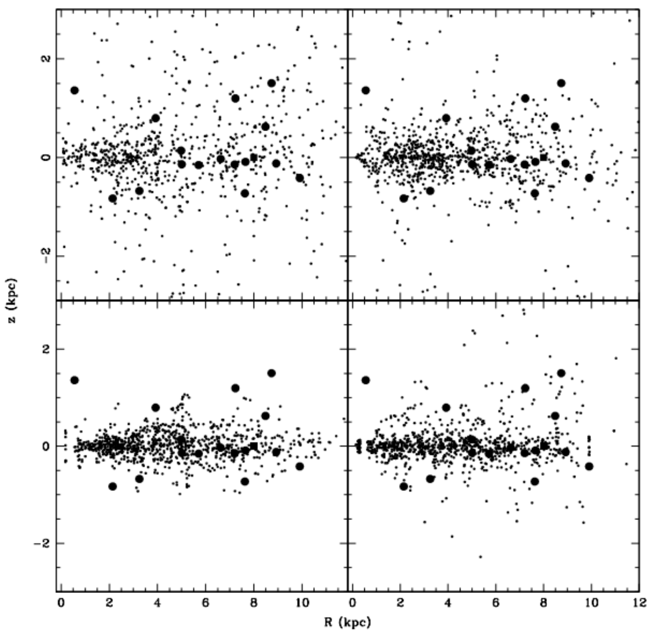

Figure 2.4: Binary population synthesis for a sample of BH-LMXBs. Top left: Hansen & Phinney distribution for natal kicks, top right: bimodal distribution, whereas the bottom figures correspond to the reduced natal kicks. Smaller dots correspond to the synthetic population, bigger ones to the observed binaries and the position of the Sun is denoted with a square (from [36]).

In order to obtain more satisfactory outcomes, it is pondered how a larger mass-loss kick would influence the conclusions. According to Eq. 2.1, mass-loss kick increases either in the case of a larger mass loss ΔM, a more compact initial binary M, or a larger companion mass M_2. By all accounts, the typical mass loss of a helium star during the SN explosion is no more than 3-4 $M_\odot$ and the orbital separation has a limiting minimum value for which either one or both of the two stars fill their Roche lobe. These considerations lead to a recoil velocity $v_{\rm mlk} \sim 40$ km/s and to a probability of exceeding 1 kpc not greater than before. By then, Repetto et al. (2012, [36]) tried to establish the minimum natal kick necessary to place the observed BH-LMXBs in their current locations, by using the parameters taken from observations. If the velocity has a direction perpendicular to the Galactic disc, the minimum kick $v_\perp$ via which the binary can travel the Galactic potential $\phi(R_0, 0)$ and reach the current position (R_0,z) is calculated as follows:

$$\frac{1}{2}v_\perp^2 + \phi(R_0, 0) = \phi(R_0, z) \tag{2.7}$$

It is revealed that for systems that are located at R $\lesssim$ 3 kpc from the Galactic center, typically required velocities are greater than 100 km/s for the highest-z systems. Clearly, these distances cannot be interpreted solely as the product of mass loss kicks: the support of BHs natal kicks (in the range $\sim$ 100-500 km/s) is required in the treatment. The larger minimum natal kick is needed for systems located close to the Galactic centre, because they must climb out of a deeper potential well.
According to theoretical models, an alternative scenario of the formation of BH binaries is due to dynamical interactions in high-density **globular clusters** (GCs). The fundamental question is whether BHs are retained in clusters or follow a different evolution. In such environments, dynamical friction contributes to decoupling black holes from the rest of the cluster and to segregating them into the core, giving birth to binaries. Subsequent dynamical interactions between these binaries and single BHs would induce the **ejection** of BHs from the cluster (where the escape velocity is $\sim$ 30-40 km/s, [15],[3]) in a timescale shorter than $\sim 10^9$ years. In case of survival, the black hole, remained in the cluster, could potentially capture a stellar companion via two main mechanisms: tidal capture of a star or exchange interactions of the BH with a binary. It is very likely that, because of tidal forces, the BH-low mass star system could end up in a merger. In general, ejections of compact-object binaries from their parent star cluster can be the result not only of dynamical ejections but also of SN kicks and GW recoil (linked to asymmetric emission). In the best-case scenario that the binary manages to escape from the cluster, it may be derived the overall distribution of Galactic BH binaries. Nonetheless, it turns out an extremely low possibility to find binaries with a GC origin, yielding to a preferable disc origin.
Comparing the synthesized population to the observed items, the best fit can be found in the model that considers BH natal kicks drawn from the same velocity distribution as for NSs. The result of Repetto et al. (2012, [36]) is quite surprising, since it was rather expected a prescription that assumes the kicks having the same momentum, i.e. where the kick velocities are reduced by the factor $(M_{\rm ns}/M_{\rm bh})$. In theoretical terms, the magnitude of the natal kick imparted to the BH depends on the competition between two timescales: the fall-back timescale $\tau_{\rm fb}$ and the timescale of the engine leading to the natal kick $\tau_{\rm nk}$. If $\tau_{\rm fb} > \tau_{\rm nk}$ (the most unrealistic case), the fall-back material would not receive the same natal kick as the proto neutron star, causing the velocity of the kick to be reduced. Otherwise, if $\tau_{\rm fb} < \tau_{\rm nk}$ the natal kick received would be full. Even though it is not possible to completely rule out the first possibility, in some cases the required natal kick exceeds the maximum kick admitted in the reduced-velocity distributions: hence, predictions from observational evidence seem to suggest the second hypothesis of a full kick.

2.3 Potential Kick Velocity distribution of BHXBs

Atri et al. (2019,[2]) aim at constraining the kicks imparted to BHXBs, in order to provide insight into the birth mechanism of BHs. They use Very Long Base Interferometry to measure proper motions of three BHXBs and combine these data with parallax, distance and systemic radial velocity (known via *Gaia*-DR2 and literature) of 16 BHXBs. In this way, the Galactocentric orbits of the three systems under investigation are determined.
In the absence of direct kick measurements, the height z of known BHXBs above the Galactic plane represents a proxy (e.g. [45],[23]) assuming the majority of the progenitors closely confined to the plane. Thanks to many simulations (as analysed in the paragraph before, [36] and [37]), it is believed the importance of natal kicks as a reason for the large displacement of several systems from the Galactic plan. They are also a deciding factor in the merging rate of BH binaries: indeed, strong natal kicks could halt the creation of binaries, by kicking single BHs out of a global cluster or by unbinding those in a binary system. Thus, although still not well constrained, the BH natal kick distribution represents a crucial parameter to insert in N-body simulations of GCs, computing the number of BHs that end up retained or ejected.
The purpose of Atri et al. (2019,[2]) is to derive the velocity of the system immediately after the BH birth. Firstly, there is the need to constrain, as best as possible, the system parameters: in particular, the three-dimensional motion of BHXBs is a key element in the attempt of inferring whether the kicks received by systems were high enough to suggest a SN origin. In this direction, the proper motion of

the BHXBs is measured and combined with the line-of-sight velocities and the distances to establish the **peculiar velocity** (i.e. the velocity of the system with respect to the local standard of rest). Nonetheless, the last-mentioned quantity could be quite deceptive for sources placed far away from the Galactic plane, since it depends on the epoch of observation and on the position inside the Galactic potential. To minimise these limitations, it is preferable to opt for the **potential kick velocity** (PKV), referring to the peculiar velocity of the system when it crosses the Galactic plane. It is thought as a better probe to understand the kick a BHXB received when the BH was born.
To draw a statistically robust scenario, the sample in consideration contains 16 BHXBs, from which Atri et al. (2019,[2]) intend to derive the PKV. Almost all BHXBs in the set have been in outburst at some point of their lifetimes: the hard X-ray spectral state is the ideal phase to conduct astrometry. The observations should be repeated after a certain amount of time, in such a way it is settled the correct baseline for measurement of proper motions.

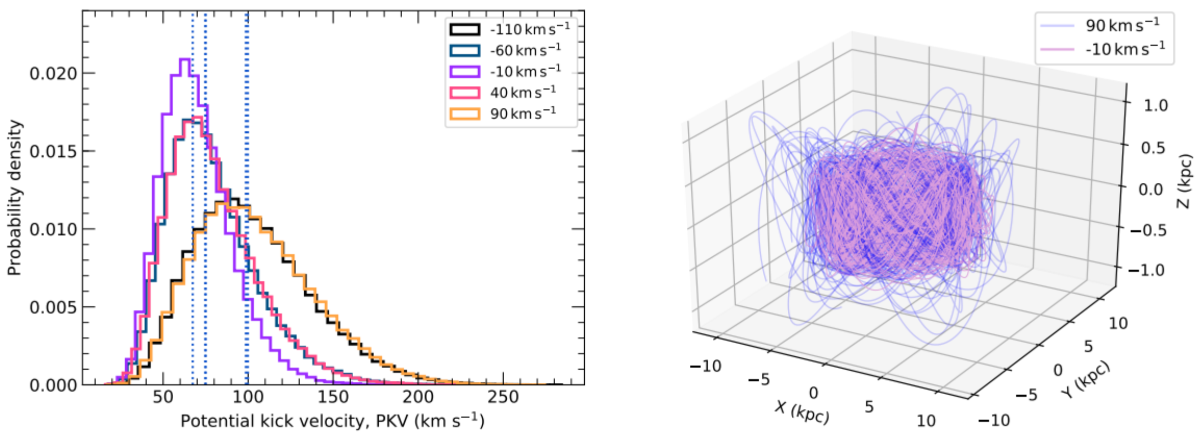

Figure 2.5: Left panel: PKV probability distribution of GRS 1716–249 using Gaussian systemic radial velocity ($\overline{\gamma}$) distributions with means of 110 km/s, -60 km/s, -10 km/s, 40 km/s and 90 km/s all with a 1σ of 50 km/s. The medians of all the PKV distributions are the blue dashed vertical lines. Right panel: a 3D visualisation of the Galactocentric orbit of GRS 1716–249, integrated for 1 Gyr for 20 orbit instances each of the lowest (67^{+41}_{-27} km/s) and highest (100^{+68}_{-47} km/s) PKV corresponding to systemic radial velocities of -10±50 km/s and 90±50 km/s, respectively. The system does not go beyond 1 kpc above the Galactic plane in both cases. (from [2]).

All the parameters have error bars associated with them, thus it is essential to propagate those errors for more accurate measurements of the peculiar velocity, via a Montecarlo (MC) methodology. Random values are picked from Gaussian distributions of the observed parameters, with standard deviation equal to the relative uncertainty. Then, these ~ 5000 random draws are used as inputs for generating Galactocentric orbits. The code integrates the trajectories for 10 Gyrs, probably exceeding the age of most of the LMXBs but not affecting the final results. The peculiar velocity at each Galactic plane crossing (meaning z=0) is estimated as indicated below:

$$v_{\text{peculiar}} = \left[(U - U_0)^2 + (V - V_0)^2 + (W - W_0)^2\right]^{0.5} \tag{2.8}$$

where U, V and W are Galactic space velocities towards the Galactic centre, in the direction of Galactic rotation and towards the North Galactic Pole respectively ([22]). U_0, V_0 and W_0 are the U, V, W components of the Galactocentric space velocities of the local standard of rest at a time when the system crosses the Galactic plane. This approach enables us to determine the **PKV probability distribution** in case proper motions of the source are known (see Figure 2.5). All four systems taken into account are provided with poorly constrained systemic radial velocities (among whom, GRS 1716–249 portrayed in Figure 2.5). With the best distance estimates, the systems are projected onto the Galactic plane: at this distance, the expected systemic radial velocity ($\overline{\gamma}$) is estimated, after assuming pure Galactic rotation around the Galactic centre. Otherwise, the last esteem is an approximation and does not properly indicate the systemic radial velocity of the system, since it may

have received kicks. Therefore, each system has been associated with five probable systemic radial velocity Gaussian distributions with medians of $\overline{\gamma}$.
Let us now try to give a physical interpretation of PKV distributions. Choosing between a unimodal or bimodal distribution (represented in the left panel of Figure 2.6) is hampered by the low number of LMXBs with constrained parameters.
If we refer to [29], stellar velocity dispersions for old systems caused by Galactic interactions are ~ 50 km/s: BHXBs are more massive, thus they suffer from lower dispersion. It is assessed that if a BHXB is endowed with a PKV exceeding 50 km/s, then the system is very likely explained via **strong kicks**. In this case, the origin of the BH in the BHXB might have been a SN explosion. Meanwhile, a median PKV less than 50 km/s suggests **weak kicks** and a formation by direct collapse. Nevertheless, low kicks could also have derived from SN explosion but been reduced due to asymmetries in the emission. It has to be stressed that the sample could be biased against detecting direct collapse BHs, since their low kicks bring them closer to the Galactic plane, where the effect of extinction is higher.

2.3.1 BH mass and spin-orbit misalignment

Efforts have been made to find a correlation between the received natal kick and the **BH mass** ([30]), extracting in this way a better understanding of the final pathway of the progenitor and the subsequent mass of the compact object. The theoretical model introduced by [41] asserts that there is no cut-off mass for direct collapse formation. Assuming BHXB PKV as a reasonable proxy for BH natal kicks distribution, Atri et al. discover a negligible relation between the BH mass and the natal kick. This seems to confirm the theory but a caveat should be made about the large error bars associated with the BH masses.

Kicks also have a significant effect on **spin-orbit misalignment** in binary systems, consisting of the angle formed between the orbital plane and the spin equator. The only evolutionary process that can effectively misalign BH spins with respect to the orbital angular momentum is the SN explosion. Spin misalignments are a possible criterion to discriminate between field binaries and star cluster binaries (e.g. [9, 10]). An isolated binary system, in which both the primary and the secondary components undergo direct collapse, is expected to end up in a BBH with nearly aligned spins. For dynamically-formed BH binaries, the typical spins are misaligned, or even nearly isotropic, because three-body encounters are able to reset any original spin alignment.
If tidal interactions could not re-align the spins, then it is predicted a high degree of misalignment. According to recent observations of GW merger events, natal kicks with speeds >50km/s are necessary to explain the phenomenon just outlined ([34]). Moreover, 90% of the sources considered by Atri et al. have PKVs greater than 50 km/s, thus the spin-orbit misalignment is extremely common in BH binaries and assigned to strongly kicked systems. There is also the evidence that realignment of the BH spin to the orbital plane is quite unusual, since its timescale in case of BHXBs is higher than the lifetime of these objects.

2.3.2 Comparison with NS kicks

To unify the treatment of BHs and NSs, it is useful to adjust a comparison between the BHXB PKV and the pulsar kick velocity distribution (Verbunt et al.,[43]). Foremost, there are some observational biases to keep in mind. Pulsars can be seen even after a strong kick has destroyed the binary they were part of, while only BHs in binaries are available in our detections. Pulsars are also usually closer, so that extinction affects less the results; furthermore, they have just two-dimensional velocities measured, making unnecessary the computation of systemic velocities.

It is evident from the previous graphic (right panel of Figure 2.6) that the medians of the two Gaussians in the BHXB PKV distribution (41 ± 14 km/s and 136 ± 17 km/s) are lower than the NS peculiar velocity peaks (120 km/s and 540 km/s) for the best fit model by a factor of 3–4. We can deduct that BHs receive **weaker natal kicks** as compared to NSs by a factor, consistent with the mass ratios of standard BHs and NSs. This conclusion is in contrast with the one presented by Repetto et al. ([36])

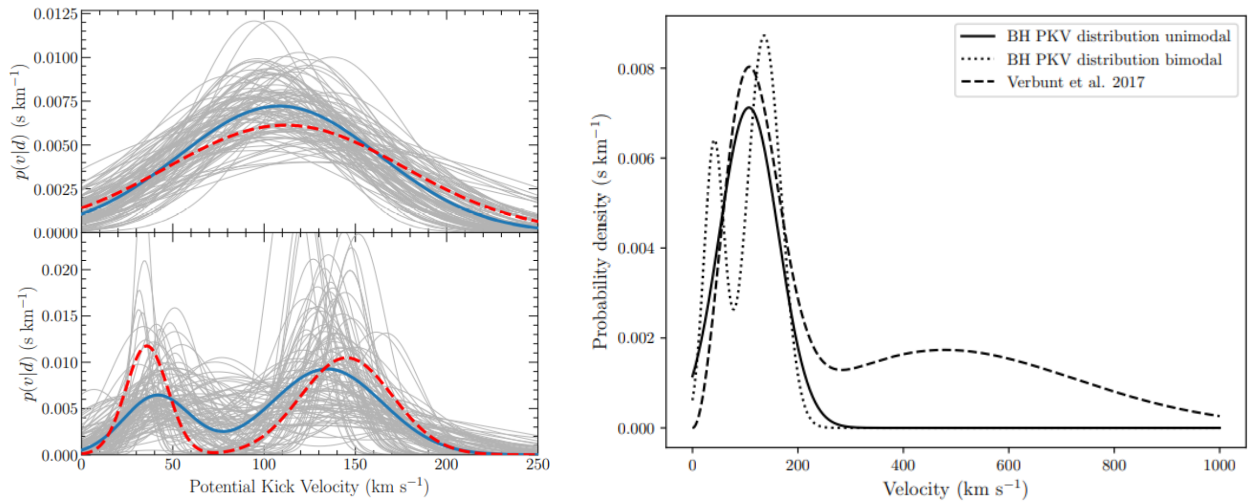

Figure 2.6: Left panel: Inferred unimodal (top) and bimodal (bottom) distributions for potential kick velocities, obtained from data. The blue lines represent the model corresponding to the median values from data of all the systems in the sample, while the red dashed lines represent the model based on the median from data of the 12 systems with systemic radial velocity constraints. The faint gray lines are a demonstration of uncertainty, coming from the MC simulations. Right panel: Comparison of best fit unimodal and bimodal BHXB PKV distributions to the best pulsar kick velocity distribution.

and described in the section above (2.2), according to which BHs and NSs receive kicks of comparable strength. As an explanation, we could either refer to the different kick mechanisms or to the biases against stronger kicks.

2.3.3 SN mass loss and z-distribution

Recalling what has been exposed in 2.1 about mass loss kick acquired after a SN explosion, we can determine the maximum possible recoil velocity $v_{\rm sys}$ due to symmetric mass loss by restricting the maximum possible mass ejected in the BHXB system, without unbinding the binary. The appropriate equation ([31]) is reported below:

$$v_{\rm sys} = 213 \left(\frac{\Delta M}{M_\odot}\right)\left(\frac{m}{M_\odot}\right)\left(\frac{P_{\text{re-circ}}}{\text{days}}\right)^{-1/3}\left(\frac{(M_{bh}+m)}{M_\odot}\right)^{-5/3} km/s \tag{2.9}$$

where ΔM, M_{bh} and m are the mass ejected, the mass of the BH and the mass of the donor after the SN, respectively. $P_{\text{re-circ}}$ is the period of the re-circularised orbit of the system after the formation of the BH (no mass transfer is assumed to occur until the re-circularisation is concluded). The PKV resulting from Atri et al. exceeds the ones predicted by [31], confirming that additional acceleration sources are needed in such systems (i.e. asymmetries in the explosion).

In earlier works (e.g. Repetto et al., [37]), the $|z|$-distribution of the distance from the Galactic plane has been declared as a good proxy in the computation of the strength of BH natal kicks. However, a system found at small height (and thus associated with a low kick) might be just caught while travelling near the Galactic plane at the current time and could spend most of their times near the orbit extrema. Consequently, a better measurement would derive from taking into consideration the **root mean square distance $z_{\rm rms}$** for comparisons between BHXBs and NSs, removing in this manner the bias of the epoch of observation and averaging the current heights. Even this treatment leads to a similar deduction as before: NSXBs are thought to obtain stronger kicks with respect to BHXBs.

3
Computations

In this chapter, we will dwell on an original series of computations and plots based upon data obtained via MOBSE (Massive Object in Binary Stellar Evolution), a population synthesis code by Giacobbo & Mapelli (2020, [13]). It represents an updated and customized version of BSE (Hurley et al. 2000, [19]). Thanks to MOBSE, the prescriptions of natal kicks presented in Section 2.1 and the simulation of a large set of both single stars and binary systems were developed.
As deepened in Subsection 1.2.1, mass loss due to stellar winds of massive hot stars is ruled by the relation $\dot{M} \propto Z^{\alpha}$: in MOBSE, α can assume the values 0.85, 2.45 - 2.4 Γ_e, and 0.05 for the electron-scattering Eddington ratio $\Gamma_e \leq 2/3$, $2/3 < \Gamma_e \leq 1$, and $\Gamma_e > 1$, respectively. The code naturally accounts for differences between ECSNe, CCSNe and ultra-stripped SNe, and includes a treatment for both pair instability and pulsation pair instability, based on Spera & Mapelli (2017, [39]). In case of pulsational pair instability, the final mass of the remnant is given by $m_{\rm rem} = \alpha_{\rm P} m_{\rm noPPI}$, where $\alpha_{\rm P}$ is a fitting parameter ([27]) and $m_{\rm noPPI}$ stands for the mass of the compact object obtained without considering pulsational pair instability (only CCSN).
Furthermore, Giacobbo & Mapelli (2020, [13]) introduce a small but fundamental difference with respect to the previous versions of MOBSE: the mass of the proto-NS in the *rapid SN explosion* model is $m_{\rm proto} = 1.1\ M_{\odot}$, whilst $m_{\rm proto}$= 1.0 $M_{\odot}$ was adopted in Fryer et al. (2012, [12]) and in the previous versions of MOBSE. Indeed, by using $m_{\rm proto}$= 1.0 $M_{\odot}$, the fraction of NSs with mass $< 1.2\ M_{\odot}$ was overestimated ([14]): then, the change of this value has permitted to match the mass of observed NSs ([42]). Other changes compared to BSE include the modelling of core radii (following [16]), the treatment of common envelope and the maximum stellar mass (extending the mass range up to 150 $M_{\odot}$, [26]). Apart from the changes recorded above, the evolution of single and binary systems in MOBSE is the one proposed by Hurley et al. (2000 [19] and 2002 [20]).

The data relative to BBHs that we plan to investigate are divided into three groups. The first set is composed of kicks drawn from the Maxwellian distribution with σ=265 km/s, coming from Hobbs et al. (2005, [18]). The second one takes into consideration kicks obtained from a Maxwellian with σ=150 km/s, a rescaling attributable to Atri et al. (2019, [2]). The last catalogue is based upon the results of Giacobbo & Mapelli (2020, [13]), where the magnitude of the kicks is given by Eq. 2.2.
Each file contained in the sets is indicated as **data_BBHs_*.txt**, where the number in place of * is the metallicity Z (i.e. the mass fraction of a star consisting of elements heavier than helium). The content of the files is explained in the header; the columns concerning our treatment are the following:

- **Col.1**: mass of the initially most massive ZAMS star (in $M_{\odot}$);
- **Col.2**: mass of the initially least massive ZAMS star (in $M_{\odot}$);
- **Col.3**: mass of the BH generated from the most massive ZAMS star (in $M_{\odot}$);
- **Col.4**: mass of the BH generated from the least massive ZAMS star (in $M_{\odot}$);
- **Col.6**: delay time, i.e. time spent between the formation of the binary and the merger of the two BHs (in Myr);
- **Col.9**: magnitude of the natal kick of the most massive ZAMS star (in km/s);
- **Col.10**: magnitude of the natal kick of the least massive ZAMS star (in km/s);

- **Col.11**: cosine of the angle between the angular momentum pre-SN and post-SN of the most massive ZAMS star;
- **Col.12**: cosine of the angle between the angular momentum pre-SN and post-SN of the least massive ZAMS star.

Our purpose is to plot some histograms of the aforementioned quantities. In this way, we can demonstrate the self-consistency of the analysed set with the theoretical prescriptions shown in the previous part of the thesis and emphasise the differences that occur between the three considered models. For ease, it has been chosen to deal with just one metallicity, Z=0.002.

3.1 ZAMS stars and BHs mass

Let us start by analysing the probability density function (PDF) of the progenitors of the compact objects, i.e. the ZAMS stars, and of the BHs originated from them and obtained via simulation. The computations have involved separately the most and the least massive stars. Among all the values at our disposal, it is clear that the ZAMS masses are the least intriguing. Nonetheless, Figures 3.1 and 3.2 consent to extract some deductions. In the treatment carried out by Hobbs and Atri, there is no dependence on the masses: the kick should be non-selective, since it operates with no dependence on the initial masses at the onset of the SN (with respect to the mass-loss kick in Eq. 2.1). In these cases, natal kicks are drawn from a Maxwellian distribution, depicted as follows:

$$P(\nu) = \nu^2 e^{\frac{-\nu^2}{2\sigma^2}} \tag{3.1}$$

where this sampling probability relies on ν, that is a given velocity component, and σ the one-dimensional root mean square. Indeed, it may be said that no great difference is found between the two distributions, having both a higher peak in correspondence of masses of $\sim$ 50-60 $M_{\odot}$ and a lower one at values slightly greater than 20 $M_{\odot}$.

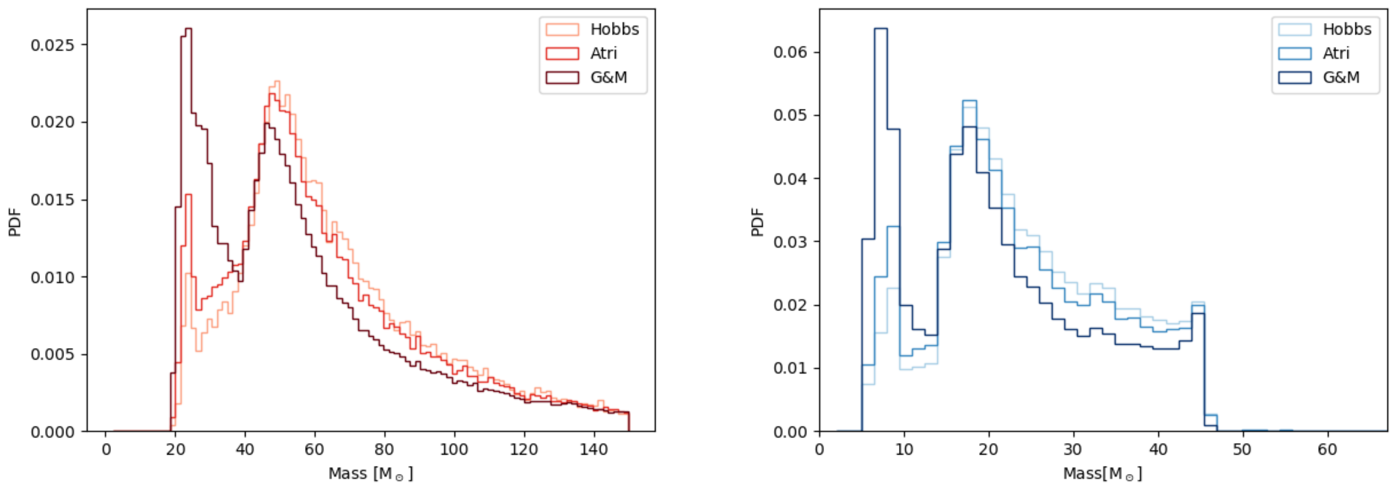

Figure 3.1: Left panel: Probability density function (PDF) of the mass of the initially most massive ZAMS star (in $M_{\odot}$). Right panel: Probability density function (PDF) of the mass of the BH generated from the least massive ZAMS star (in $M_{\odot}$).

Instead, a more sophisticated prescription elaborated by Giacobbo & Mapelli (2020,[13]) considers also the role played by the ejected mass $m_{\rm ej}$. The most populated ZAMS mass stands at around 20 $M_{\odot}$; another peak that appears lower with respect to the latter and to the other distributions is at $\gtrsim$ 50 $M_{\odot}$. The mass distribution of the resulting BHs is almost the same for the three models, covering a range from $\sim$ 5 to less than 60 $M_{\odot}$. However, even in this case, the lower values in the plot

corresponding to Giacobbo & Mapelli leap to the eye. This visual is readily explained because objects endowed with lower masses and subject to mass loss via ejection are more likely to survive in a bound binary (which later ends up in coalescence) as compared to higher masses. The same propensity is evident in the ZAMS mass distributions: the high kick velocities (σ=265 km/s in Hobbs, while σ=150 km/s in Atri) support greater masses, both for the ZAMS stars and the remnants.
We can reach nearly the same conclusion for the least massive ZAMS stars and the associate BHs in the simulation (see Figure 3.2). In the left panel, it is less evident the prevalence of lower masses for the model introduced by Giacobbo & Mapelli: the data portrayed seem to suggest a unimodal distribution for all three prescriptions, with the highest peak at $\sim$ 20 km/s and at $\sim$ 40 km/s, for Giacobbo & Mapelli (hereafter, G&M) and Hobbs and Atri, respectively. The BHs mass distribution presents a prominent value around 10 $M_{\odot}$ for G&M and another one at $\lesssim$ 50 $M_{\odot}$, confirming the trend exposed above.

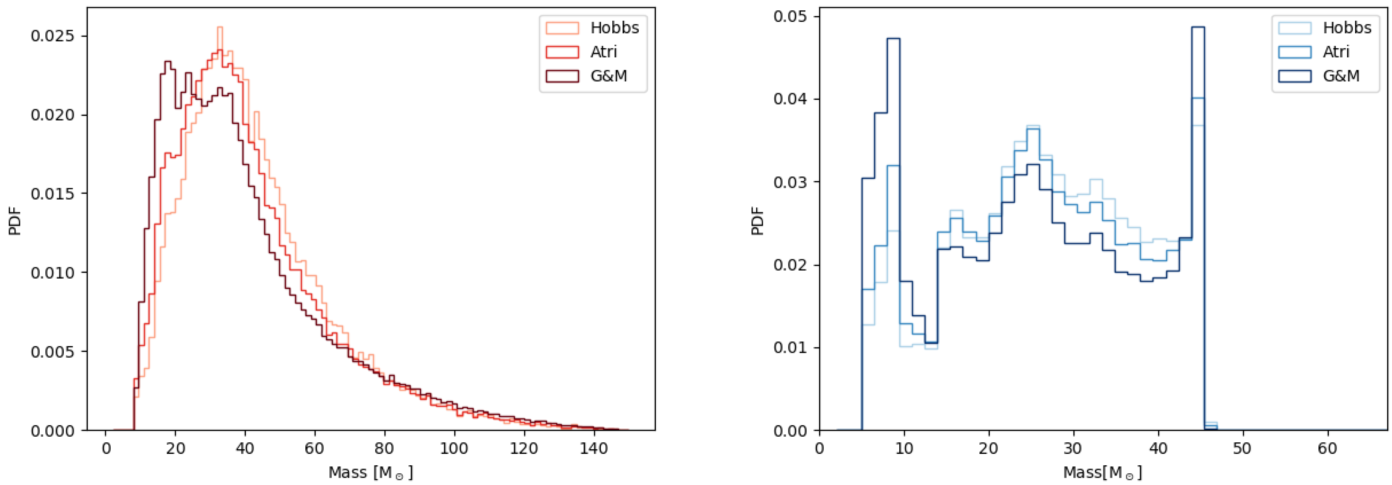

Figure 3.2: Left panel: Probability density function (PDF) of the mass of the initially most massive ZAMS star (in $M_{\odot}$). Right panel: Probability density function (PDF) of the mass of the BH generated from the initially least massive ZAMS star (in $M_{\odot}$).

3.2 Delay Time

From now on, we will investigate the delay time, i.e. the time spent from the formation of the binary system (at t=0 of the simulation) to the coalescence via GW emission. The computation of this quantity implicates outlining the physics, that rules over the phases pre- and post-BBH birth. After the binary is established, it may be predicted the lifetime of the system for collapse as a result of the radiation of gravitational waves, by using the premises of General Relativity. Following Peters (1964, [35]), we consider the case of circularly orbiting binary stars for which we neglect deformation, mass flow, and other radiation processes. In a bound system of two point masses moving in elliptical orbits, the secular decays of the semi-major axis and eccentricity are found as functions of time, and are integrated to specify the decay by gravitational radiation of such systems as functions of their initial conditions. A numerical solution to the **coalescence time** in case of a circular orbit (e =0), is given by [35]:

$$T_c(a_0) = \frac{a_0^4}{4\beta} \tag{3.2}$$

where a_0 is the semi-major axis at the time of the observation and β is a factor which depends to G the universal gravitational constant, c the speed of light and m_1, m_2 the masses that compose the binary in a close orbit around a common centre of gravity:

$$\beta = \frac{64G^3 m_1 m_2 (m_1 + m_2)}{5c^5} \tag{3.3}$$

In other works (e.g. Nyadzani et al.,[32]), it is presented an analytical estimate of the coalescence time of a binary system with an arbitrary eccentricity 0< e_0 <1 and a semi-major axis a_0 at the time of observation. Indeed, in the general case, with arbitrary values of a and e, the coalescence time can be calculated by solving the coupled time derivatives of a and e together. A widely used analytical approximation of the coalescence time was calculated by Shapiro et al. (1983, [38]) as:

$$T_m(a_0, e_0) = T_c(a_0)\frac{(1-e_0^2)^{7/2}}{(1+\frac{73}{24}e_0^2+\frac{37}{96}e_0^4)} \tag{3.4}$$

Holding these theoretical tools, it is possible to interpret the data collected in our observational set (see Figure 3.3). It is visible in the plot the power law followed by the delay times taken into consideration: the evolution of the time-scale obeys to an **exponentially-decreasing** model, starting from $t_{\text{del}} = 0$ until $t_{\text{del}} \simeq 150$ Myr.

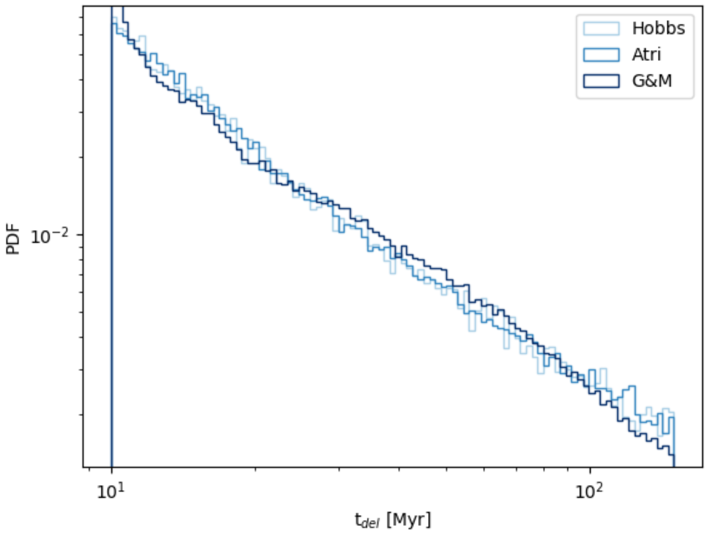

Figure 3.3: Probability density function (PDF) in logarithmic scale of the delay time, that occurs between the formation and the coalescence of the binary system.

The tendency for these systems to prefer **lower delay times** could be explained by recurring to the more complicated physics behind the kicks and the ultimate phases before the definitive formation of the binary. Higher kicks actually have a threshold effect, either on the birth or on the disruption of binary systems: if sufficiently elevated, they are able to split the orbit of the two objects, which will continue the rest of their lifetimes as single entities. In the best-case scenario, a *"lucky"* kick takes part in increasing the eccentricity, whilst the binary remains bound. To understand the trend pinned down in the plot, it is useful to highlight from Eq. 3.2 and 3.4 the main dependencies, assuming for simplicity $m_1 \approx m_2 = m$:

$$T_{\text{delay}} \propto a_0^4 \frac{1}{m^3}(1-e_0)^{7/2} \tag{3.5}$$

Consequently, the low values of delay time depicted could occur due to high eccentricities, short orbital separation and huge masses in circulation: then, these conditions might lead to a merger between the two BHs in a brief period. The orbital properties are heavily influenced by the mechanism of the kicks. On the other hand, the final masses of the BHs involved change if considering one model despite another. In fact, it is deducted from the graphic that Hobbs (and, to a lesser degree, also Atri) incorporates delay times shorter with respect to G&M. A reason can be found in having considered the impact of the ejected mass during the SN explosion in the treatment by G&M, fostering lower masses and thus longer delay times.

3.3 Magnitude of the kicks

At this point, let us show the histograms relative to the magnitude of the kicks and verify their consistency with the various distributions presented along the thesis. The graphics (Figures 3.4) suggest a trend toward **smaller kicks** compared to the average predictions. The model by G&M presents a peak at around $\sim$ 10 km/s: therefore, the velocity appears highly suppressed, because it has been implemented as indicated below.

$$v_{\text{kick}} = (1 - f_{\text{fb}}) f_{\text{H05}} \tag{3.6}$$

where f_{H05} is a random number drawn from the Maxwellian distribution with σ=265 km/s. Clearly, since the velocities calculated with Eq. 3.6 are corrected for the amount of fallback, they are reduced as against those computed by Hobbs and Atri. In general, binary evolution tends to increase the number of BHs with lower kicks, because dissipative mass transfer tends to reduce m_{ej} (see also Eq. 2.2).
The other distributions do not deviate that far from the ones predicted by the theory, with the higher values reached being $\sim$ 160 km/s and $\sim$ 280 km/s, for Hobbs and Atri respectively. A remark is that they seem flattened in the amount of data provided. Nonetheless, it is necessary to point out that reasonably the distributions will not be the same as the originals. This is because the BHs generated in the simulations and then studied are solely the survivors of the mechanisms of explosion: the orbits of the progenitors might be widened or disrupted by $\sim$ 100 km/s natal kicks, and only a small fraction remains inside a bound binary.

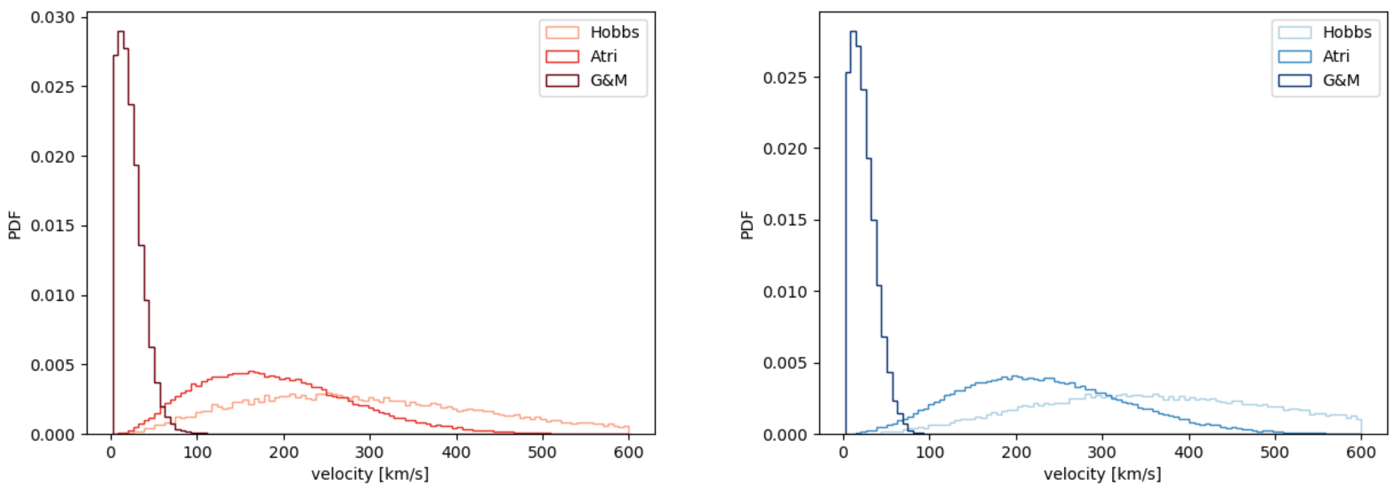

Figure 3.4: Left panel: Probability density function (PDF) of the magnitude of the kicks, which affect the initially more massive ZAMS stars (in km/s). Right panel: Probability density function (PDF) of the magnitude of the kicks, which affect the initially less massive ZAMS stars (in km/s).

3.4 BHs angular momentum

In this last section, we report the graphics relative to $\cos\alpha$, where α is the angle formed between the angular momentum before and after the explosion of the SN (see Figures 3.5). In Subsection 2.3.1, it has been already discussed about the high possibility for compact objects to inherit a **spin-orbit misalignment** after dynamical interactions. In general (e.g. [5]), it is helpful to compare the correlations between various orbital parameters with observational samples to yield information about kick velocities and pre-SN orbital-period distributions. After the SN, the spins of most stars in massive systems have **large inclinations** with respect to their orbital axes, and a significant fraction of systems ($\sim$ 20 %) contain stars with retrograde spins. Systems that suffer stronger natal kicks have generally higher space velocities and are more likely to have misaligned spin axes in relation to their orbital axes. According to [5], the angle α of the post-SN orbital angular momentum vector with respect to the initial orbital angular momentum vector can be written as:

$$\cos\alpha = \frac{1 + \tilde{v}\cos\phi\cos\theta}{[\tilde{v}^2 \sin\theta^2 + (1 + \tilde{v}\cos\phi\cos\theta)]^{1/2}} \tag{3.7}$$

where $\tilde{v} = v_{\rm kick}/v_{\rm orb}$ is the ratio between the velocity of the kick and the magnitude of the initial relative orbital velocity. The direction of the kick is specified by two angles: θ indicates the angle between the direction of the $v_{\rm kick}$ vector and the initial orbital plane, while ϕ is formed between the initial direction of motion of the star (which experiences the SN) and the projection of the $v_{\rm kick}$ vector on to the orbital plane. The spins are retrograde with respect to the orbital motion if $v > 90°$. Unfortunately, the angles θ and ϕ are particularly hard to measure using current detectors. However, LIGO and Virgo allow to give an estimate of two spin combinations, i.e. the effective spin ($\chi_{\rm eff}$) and the precessing spin ($\chi_{\rm p}$). The effective spin is expressed as:

$$\chi_{\rm eff} = \frac{(m_1\chi_1 + m_2\chi_2)}{m_1 + m_2} \cdot \frac{\mathbf{L}}{L} \tag{3.8}$$

where m_1 and m_2 (χ_1 and χ_2) are the masses (dimensionless spin parameters) of the primary and secondary component of the binary, respectively and $\mathbf{L}$ is the Newtonian orbital angular momentum vector of the binary.

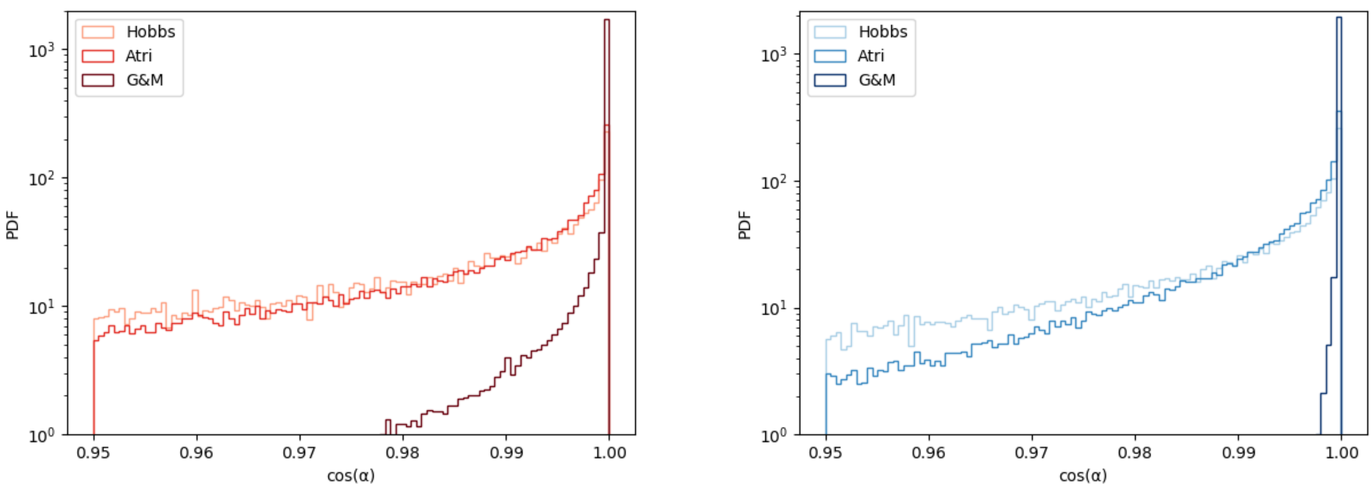

Figure 3.5: Left panel: Probability density function (PDF) of $\cos\alpha$ in logarithmic scale, where α is the angle formed by the angular momentum pre- and post-SN affecting the initially more massive ZAMS stars. Right panel: Probability density function (PDF) of $\cos\alpha$, where α is the angle formed by the angular momentum pre- and post-SN affecting the initially more massive ZAMS stars.

From Fig. 3.5, we can extract some information: it has been found that the BHs in the simulation reveal values of $\cos\alpha$ almost equal to 1, for the vast majority, for α created between pre- and post-SN phase (both for the most and least massive stars in the set). Nevertheless, the reasons behind the two scenarios are very different from one another. Before the explosion takes place, there is the possibility for the isolated binary to own nearly aligned spins: this could suggest thinking of the angles α formed by the angular momentum as very small. Afterwards, the dynamic of the kicks plays its role, triggering in most cases the aforementioned spin-orbit misalignment: the higher the kick velocity, the greater the angle difference will be. Consequently, the largest angles are deeply connected to the observations via GWs of several BBH systems with spins tilted by more than 90° with respect to their orbital angular momentum.

4

Conclusions

The aim of the thesis was to portray an exhaustive scenario of the **natal kicks**, which could affect binary black holes: a phenomenon that appears still not fully comprehended. It concerns the physical mechanisms that operate between the ultimate events of the life of a massive star and the final formation of a compact object. In particular, some of the episodes that follow the creation of a BH and then the entering into a binary system remain involved in uncertainties. Attempts have been made in order to shed some light on a field yet to be explored. Towards this direction, we started by reviewing the main steps made in **gravitational wave** astrophysics: the most accurate observations have been reached recently, thanks to the interferometers LIGO and Virgo. The detections allow to provide us with the first evidence of the merging of a binary system, as it was predicted a century ago by Albert Einstein in General Relativity. Later on, we have lingered on the formation of BHs from single stellar evolution, by considering them as isolated systems. It is of great significance to mark the threshold mass of the dying star, which determines whether the compact remnant would be a NS or a BH. Therefore, the main processes that characterised the ultimate phases of massive stars have been briefly shown. The envelope of the progenitors, for example, could evaporate due to stellar winds or mass transfer if the binary is caught inside a common envelope. Then, we explored the collapse of the core and the main triggers of the instability: in order to clarify the physics of the SN, the convective engine and the role played by neutrinos have been examined.
Hereinafter, we tackled the main argument of the thesis, presenting state-of-the-art knowledge about natal kicks and deepening, in specific, the effect on BHs evolution. Firstly, we analysed the useful background to quantitatively measure the strength of the kicks, starting from the discrimination between BHs born from fallback and those from direct collapse. Thereby, we wanted to determine to what extent the BHs are influenced in their pathways, depending on, for instance, how the orbital properties and the merger rate can change. Along these lines, three works have been reviewed, each one focusing on a different aspect of the phenomenon via **population synthesis simulations**. The main purpose was to find the distribution of the kick velocities, which fits better with both observational data and theoretical perspective. Among the possible methods to measure the magnitude of the kick, it has been developed the study of the location of binaries within the Galaxy: strong kicks are naturally responsible for large heights recorded above the Galactic plane. The best probes at our disposal are **black hole X-ray binaries**, since it is difficult to observe binaries of stellar BHs: thus, the interferometers have furnished proper motion measurement, in order to get the peculiar velocity of the system in respect to the local standard of rest. In this regard, we tried to find out what velocity should the compact object inherit to reach its current position and from what kind of environment and interactions the BH originated. It is clear that each sample made progress in a certain direction. Even though an overall framework is slowly emerging, certainties are still missing: indeed, it is tough to integrate the different views proposed by the prescriptions, as has been proven somehow in the original part of this thesis. There is no self-consistent scenario that captures the complex physics of SNe: one model apparently works better on low-mass stars as progenitors of BHs, while others seem to match with the most massive stars of the set. These results suggest that a **further investigation** of the details of natal kick impact on a system is needed, by considering a larger sample of binaries. The number of GW events detected so far is still too low to put robust constraints on the parameters involved. In addition to that, all the equations reported, as well as the ones used in the population-synthesis codes suffer from several approximations. On one side, we underlined how crucial natal kicks are in the complete understanding of BBH evolution. Still, it is an open issue in anticipation of the upcoming runs of LIGO and Virgo.

References

[1] Z. Arzoumanian, D. F. Chernoff, and J. M. Cordes. "The Velocity Distribution of Isolated Radio Pulsars". In: 568.1 (Mar. 2002), pp. 289–301. DOI: 10.1086/338805. arXiv: astro-ph/0106159 [astro-ph].

[2] P Atri et al. "Potential kick velocity distribution of black hole X-ray binaries and implications for natal kicks". In: *Monthly Notices of the Royal Astronomical Society* 489.3 (Aug. 2019), pp. 3116–3134. DOI: 10.1093/mnras/stz2335. URL: https://doi.org/10.1093%2Fmnras%2Fstz2335.

[3] Krzysztof Belczynski et al. "Compact Object Modeling with the StarTrack Population Synthesis Code". In: *The Astrophysical Journal Supplement Series* 174.1 (Jan. 2008), pp. 223–260. DOI: 10.1086/521026. URL: https://doi.org/10.1086%2F521026.

[4] A. Blaauw. "On the origin of the O- and B-type stars with high velocities (the "run-away" stars), and some related problems". In: 15 (May 1961), p. 265.

[5] W. N. Brandt and Ph. Podsiadlowski. *The Effects of High-Velocity Supernova Kicks on the Orbital Properties and Sky Distributions of Neutron Star Binaries*. 1994. DOI: 10.48550/ARXIV.ASTRO-PH/9412023. URL: https://arxiv.org/abs/astro-ph/9412023.

[6] J C Bray and J J Eldridge. "Neutron star kicks – II. Revision and further testing of the conservation of momentum 'kick' model". In: *Monthly Notices of the Royal Astronomical Society* 480.4 (Aug. 2018), pp. 5657–5672. DOI: 10.1093/mnras/sty2230. URL: https://doi.org/10.1093%2Fmnras%2Fsty2230.

[7] J. C. Bray and J. J. Eldridge. "Neutron star kicks and their relationship to supernovae ejecta mass". In: *Monthly Notices of the Royal Astronomical Society* 461.4 (May 2016), pp. 3747–3759. DOI: 10.1093/mnras/stw1275. URL: https://doi.org/10.1093%2Fmnras%2Fstw1275.

[8] T. Ertl et al. "A two-parameter criterion for classifying the explodability of massive stars by the neutrino-driven mechanism". In: *The Astrophysical Journal* 818.2 (Feb. 2016), p. 124. DOI: 10.3847/0004-637x/818/2/124. URL: https://doi.org/10.3847%2F0004-637x%2F818%2F2%2F124.

[9] Ben Farr, Daniel E. Holz, and Will M. Farr. "Using Spin to Understand the Formation of LIGO and Virgo's Black Holes". In: *The Astrophysical Journal* 854.1 (Feb. 2018), p. L9. DOI: 10.3847/2041-8213/aaaa64. URL: https://doi.org/10.3847%2F2041-8213%2Faaaa64.

[10] Will M. Farr et al. "Distinguishing spin-aligned and isotropic black hole populations with gravitational waves". In: *Nature* 548.7668 (Aug. 2017), pp. 426–429. DOI: 10.1038/nature23453. URL: https://doi.org/10.1038%2Fnature23453.

[11] Chris Fryer, Adam S. Burrows, and W. Benz. "Population Syntheses for Neutron Star Systems with Intrinsic Kicks". In: *The Astrophysical Journal* 496 (1998), pp. 333–351.

[12] Chris L. Fryer et al. "Compact remnant mass function: dependence on the explosion mechanism and metallicity". In: *The Astrophysical Journal* 749.1 (Mar. 2012), p. 91. DOI: 10.1088/0004-637x/749/1/91. URL: https://doi.org/10.1088%2F0004-637x%2F749%2F1%2F91.

[13] Nicola Giacobbo and Michela Mapelli. "Revising Natal Kick Prescriptions in Population Synthesis Simulations". In: *The Astrophysical Journal* 891.2 (Mar. 2020), p. 141. DOI: 10.3847/1538-4357/ab7335. URL: https://doi.org/10.3847%2F1538-4357%2Fab7335.

[14] Nicola Giacobbo and Michela Mapelli. "The progenitors of compact-object binaries: impact of metallicity, common envelope and natal kicks". In: *Monthly Notices of the Royal Astronomical Society* 480.2 (July 2018), pp. 2011–2030. DOI: 10.1093/mnras/sty1999. URL: https://doi.org/10.1093%2Fmnras%2Fsty1999.

[15] Oleg Y. Gnedin et al. "The Unique History of the Globular Cluster ω Centauri". In: *The Astrophysical Journal Letters* 568 (2002), pp. L23–L26.

[16] Philip D. Hall and Christopher A. Tout. "Core radii and common-envelope evolution". In: *Monthly Notices of the Royal Astronomical Society* 444.4 (Sept. 2014), pp. 3209–3219. DOI: 10.1093/mnras/stu1678. URL: https://doi.org/10.1093%2Fmnras%2Fstu1678.

[17] Brad M. S. Hansen and E. Sterl Phinney. “The pulsar kick velocity distribution”. In: 291.3 (Nov. 1997), pp. 569–577. DOI: 10.1093/mnras/291.3.569. arXiv: astro-ph/9708071 [astro-ph].

[18] G. Hobbs et al. “A statistical study of 233 pulsar proper motions”. In: *Monthly Notices of the Royal Astronomical Society* 360.3 (July 2005), pp. 974–992. DOI: 10.1111/j.1365-2966.2005.09087.x. URL: https://doi.org/10.1111%2Fj.1365-2966.2005.09087.x.

[19] J. R. Hurley, O. R. Pols, and C. A. Tout. “Comprehensive analytic formulae for stellar evolution as a function of mass and metallicity”. In: *Monthly Notices of the Royal Astronomical Society* 315.3 (July 2000), pp. 543–569. DOI: 10.1046/j.1365-8711.2000.03426.x. URL: https://doi.org/10.1046%2Fj.1365-8711.2000.03426.x.

[20] Jarrod R. Hurley, Christopher A. Tout, and Onno R. Pols. “Evolution of binary stars and the effect of tides on binary populations”. In: *Monthly Notices of the Royal Astronomical Society* 329.4 (Feb. 2002), pp. 897–928. DOI: 10.1046/j.1365-8711.2002.05038.x. URL: https://doi.org/10.1046%2Fj.1365-8711.2002.05038.x.

[21] Hans-Thomas Janka. “Explosion Mechanisms of Core-Collapse Supernovae”. In: *Annual Review of Nuclear and Particle Science* 62.1 (Nov. 2012), pp. 407–451. DOI: 10.1146/annurev-nucl-102711-094901. arXiv: 1206.2503 [astro-ph.SR].

[22] Dean R. H. Johnson and David R. Soderblom. “Calculating Galactic Space Velocities and Their Uncertainties, with an Application to the Ursa Major Group”. In: 93 (Apr. 1987), p. 864. DOI: 10.1086/114370.

[23] P. G. Jonker and G. Nelemans. “The distances to Galactic low-mass X-ray binaries: consequences for black hole luminosities and kicks”. In: 354.2 (Oct. 2004), pp. 355–366. DOI: 10.1111/j.1365-2966.2004.08193.x. arXiv: astro-ph/0407168 [astro-ph].

[24] M. Mapelli et al. “Dynamics of stellar black holes in young star clusters with different metallicities – I. Implications for X-ray binaries”. In: *Monthly Notices of the Royal Astronomical Society* 429.3 (Jan. 2013), pp. 2298–2314. DOI: 10.1093/mnras/sts500. URL: https://doi.org/10.1093%2Fmnras%2Fsts500.

[25] Michela Mapelli. *Formation channels of single and binary stellar-mass black holes.* June 2021.

[26] Michela Mapelli. “Massive black hole binaries from runaway collisions: the impact of metallicity”. In: *Monthly Notices of the Royal Astronomical Society* 459.4 (Apr. 2016), pp. 3432–3446. DOI: 10.1093/mnras/stw869. URL: https://doi.org/10.1093%2Fmnras%2Fstw869.

[27] Michela Mapelli et al. “Impact of the Rotation and Compactness of Progenitors on the Mass of Black Holes”. In: *The Astrophysical Journal* 888.2 (Jan. 2020), p. 76. DOI: 10.3847/1538-4357/ab584d. URL: https://doi.org/10.3847%2F1538-4357%2Fab584d.

[28] Paola Marigo. *Theoretical Astrophysics, lecture notes.*

[29] F. Mignard. “Local galactic kinematics from Hipparcos proper motions”. In: 354 (Feb. 2000), pp. 522–536.

[30] Félix Mirabel. “The formation of stellar black holes”. In: *New Astronomy Reviews* 78 (Aug. 2017), pp. 1–15. DOI: 10.1016/j.newar.2017.04.002. URL: https://doi.org/10.1016%2Fj.newar.2017.04.002.

[31] G. Nelemans, T. M. Tauris, and E. P. J. van den Heuvel. “Constraints on Mass Ejection in Black Hole Formation Derived from Black Hole X-Ray Binaries”. In: *Black Holes in Binaries and Galactic Nuclei: Diagnostics, Demography and Formation.* Ed. by Lex Kaper, Edward P. J. van den Heuvel, and Patrick A. Woudt. Berlin, Heidelberg: Springer Berlin Heidelberg, 2001, pp. 312–313. ISBN: 978-3-540-44562-3.

[32] Lutendo Nyadzani and Soebur Razzaque. *Coalescence Time of Compact Binary Systems.* 2019. DOI: 10.48550/ARXIV.1905.06086. URL: https://arxiv.org/abs/1905.06086.

[33] Evan O’Connor and Christian D. Ott. “Black Hole formation in failing core-collapse Supernovae”. In: *The Astrophysical Journal* 730.2 (Mar. 2011), p. 70. DOI: 10.1088/0004-637x/730/2/70. URL: https://doi.org/10.1088%2F0004-637x%2F730%2F2%2F70.

[34] Richard O’Shaughnessy, Davide Gerosa, and Daniel Wysocki. “Inferences about Supernova Physics from Gravitational-Wave Measurements: GW151226 Spin Misalignment as an Indicator of Strong Black-Hole Natal Kicks”. In: *Physical Review Letters* 119.1 (July 2017). DOI: 10.1103/physrevlett.119.011101. URL: https://doi.org/10.1103%2Fphysrevlett.119.011101.

[35] P. C. Peters. "Gravitational Radiation and the Motion of Two Point Masses". In: *Phys. Rev.* 136 (4B Nov. 1964), B1224–B1232. DOI: 10.1103/PhysRev.136.B1224. URL: https://link.aps.org/doi/10.1103/PhysRev.136.B1224.

[36] Serena Repetto, Melvyn B. Davies, and Steinn Sigurdsson. "Investigating stellar-mass black hole kicks". In: *Mon. Not. Roy. Astron. Soc.* 425 (2012), p. 2799. DOI: 10.1111/j.1365-2966.2012.21549.x. arXiv: 1203.3077 [astro-ph.GA].

[37] Serena Repetto, Andrei P. Igoshev, and Gijs Nelemans. "The Galactic distribution of X-ray binaries and its implications for compact object formation and natal kicks". In: *Monthly Notices of the Royal Astronomical Society* 467 (2017), pp. 298–310.

[38] S. L. Shapiro, S. A. Teukolsky, and Alan P. Lightman. "Black Holes, White Dwarfs, and Neutron Stars: The Physics of Compact Objects". In: *Physics Today* 36.10 (Jan. 1983), p. 89. DOI: 10.1063/1.2915325.

[39] Mario Spera and Michela Mapelli. "Very massive stars, pair-instability supernovae and intermediate-mass black holes with the sevn code". In: *Monthly Notices of the Royal Astronomical Society* 470.4 (June 2017), pp. 4739–4749. DOI: 10.1093/mnras/stx1576. URL: https://doi.org/10.1093%2Fmnras%2Fstx1576.

[40] Mario Spera et al. "Merging black hole binaries with the SEVN code". In: *Monthly Notices of the Royal Astronomical Society* 485.1 (Feb. 2019), pp. 889–907. DOI: 10.1093/mnras/stz359. URL: https://doi.org/10.1093%2Fmnras%2Fstz359.

[41] Tuguldur Sukhbold et al. "Core-Collapse Supernovae from 9 to 120 solar masses based on neutrino-powered explosion". In: *The Astrophysical Journal* 821.1 (Apr. 2016), p. 38. DOI: 10.3847/0004-637x/821/1/38. URL: https://doi.org/10.3847%2F0004-637x%2F821%2F1%2F38.

[42] T. M. Tauris et al. "Formation of Double Neutron Star Systems". In: *The Astrophysical Journal* 846.2 (Sept. 2017), p. 170. DOI: 10.3847/1538-4357/aa7e89. URL: https://doi.org/10.3847%2F1538-4357%2Faa7e89.

[43] Theo F. J. van Grunsven et al. "The mass of the black hole in 1A 0620-00, revisiting the ellipsoidal light curve modelling". In: 472.2 (Dec. 2017), pp. 1907–1914. DOI: 10.1093/mnras/stx2071. arXiv: 1708.08209 [astro-ph.HE].

[44] R. F. Webbink. "Double white dwarfs as progenitors of R Coronae Borealis stars and type I supernovae." In: 277 (Feb. 1984), pp. 355–360. DOI: 10.1086/161701.

[45] Nicholas White and Paradijs. "The Galactic Distribution of Black Hole Candidates in Low-Mass X-Ray Binary Systems". In: *The Astrophysical Journal Letters* 473 (Jan. 2009), p. L25. DOI: 10.1086/310380.

[46] S. E. Woosley, A. Heger, and T. A. Weaver. "The evolution and explosion of massive stars". In: *Rev. Mod. Phys.* 74 (4 Nov. 2002), pp. 1015–1071. DOI: 10.1103/RevModPhys.74.1015. URL: https://link.aps.org/doi/10.1103/RevModPhys.74.1015.